# The inter-annual variability in the onset of the enhanced chlorophyll-a east of Madagascar

Oozeeraully Yuneeda Bibi Naheed

OZRYUN001

Supervisors: Professor Chris Reason, Dr. Juliet Hermes &Dr.Charine Collins

---

Minor dissertation

Submitted in partial fulfilment of the requirements for the degree of Master of Science in Applied Marine Science

Department of Biological Sciences
Faculty of Science
University of Cape Town

---

**February 2015**

## Plagiarism declaration

I know the meaning of plagiarism and declare that all of the work in the dissertation, save for that which is properly acknowledged, is my own. Aside from guidance from my supervisors, I have received no assistance, except as acknowledged.

SIGNATURE: _____

DATE: _____

## Acknowledgements

Firstly, I would like to thank my Dad and Mum and my sister, Yushrina, for their unconditional love, patience and support during the good and bad times. This venture would not have been possible without them and I would like to whole-heartedly thank them.

I would like to thank my supervisors, Professor Chris Reason, Dr. Juliet Hermes and Dr. Charine Collins for their constant support, guidance and encouragement throughout this project. I am also grateful to them for always being here for me whenever I encountered any difficulties.

Special thanks to Dr. Charine Collins who provided me with the data and for her patience with my countless Matlab questions. I would also like to thank Fehmi Dilmahamod for his help, patience and for our valuable discussions we had on the topic. I would like to express my gratitude to Associate Professor Marcello Vichi for his help with Matlab.

Thank you to all my friends, Daneeja, Lekraj, Bhavnah and classmates from AMS for their kindness, support, company and for making this year a memorable one. It has been one of the best experiences in my life.

Lastly, I would like to acknowledge the Marine Research Institute (Ma-Re) for the partial funding for this project.

# Abstract

Chlorophyll-a concentration is a measure of phytoplankton biomass and is therefore used as a proxy for primary production. The chlorophyll bloom occurring in the South western Indian Ocean is one of the major blooms in the open ocean and is subject to controversies about its formation, propagation and termination mechanisms. In this study, the region was divided into two sub-regions, the South East region (48°E-66°E, 24°S-30°S) and the East region (70°E-88°E, 24°S-30°S) and satellite datasets of chlorophyll-a, sea surface temperature, wind speed and direction and sea surface height were analysed. A bloom was characterized by twice the mean level of the sub-region (~0.08mg/$m^3$) and three bloom years were identified: 2004, 2006 and 2008. The timing, propagation and termination of the bloom showed spatial and temporal variability. The wavelet analysis revealed a semi-annual signal for 2006 and 2008 and an annual one in 2004 due to the gradual decline in the concentration of chlorophyll-a. The transport of the bloom is affected by the passage of eddies where the concentration of chlorophyll-a is higher in the core and around the edges in cyclonic and anti-cyclonic eddies respectively. The bloom could be present at the sub-surface level throughout the years but is only apparent at the surface during specific years.

## Table of Contents

## List of Figures

## List of Tables

# 1. Introduction

The bloom occurring southeast of Madagascar is one of the largest dendroid blooms in the world oceans. Its largest extent can cover approximately 1% of the world's ocean surface area (Srokosz and Quartly, 2013). It is one of the strongest examples of inter-annual variability in ocean biology after El Niño and must have ramifications for the biogeochemistry of the basin (Uz, 2007). Understanding the physical oceanography of the region is key to better understanding the processes forming the phytoplankton bloom.

Several studies have addressed the different mechanisms controlling the formation, propagation and termination of the bloom, but there are many questions still unanswered. Raj et al. (2010) explored a variety of long-term data sets and found that upwelling along the south Madagascar coast, precipitation along east Madagascar, and mesoscale eddies were likely to be key factors influencing the bloom. Huhn et al. (2012) used altimeter and hydrographic data to show that there was a narrow shallow eastward propagating zonal jet, known as the Southern Indian Ocean Counter-current (Siedler et al., 2006; Palastanga et al., 2007; Nauw et al., 2008). The SICC runs along 25°S, the latitude where the Madagascar plankton bloom typically develops (Huhn et al., 2012). Zonal jets can behave as meridional transport barriers (Beron-Vera et al., 2008, 2010; Shuckburgh et al., 2009) and thus contribute to the shaping of plankton bloom distributions. However, the details of the transport mechanisms still remain unclear (Huhn et al., 2012).

Previous reports have discrepancies in explaining the period of onset of the bloom. While, Longhurst (2001) reported the bloom to develop in January, Uz (2007) reported its onset during February or March. Lévy et al. (2007) reported that the bloom starts in November-December and that its largest extent is reached in February or March in most years. Uz (2007) showed that the bloom tends to develop in years when tropical cyclones make landfall

in Madagascar and suggested that the runoff of iron from the island triggers the onset of the bloom. However, traces of a weak bloom were observed in the Madagascar Basin during 2005, even though the number of cyclones hitting the Madagascar coast during the year was at its lowest compared to all other non-bloom years (Uz, 2007). This questions the adequacy of the hypothesis of bio-availability of iron alone in explaining the inter-annual variability of the phytoplankton bloom in the South Western Indian Ocean (Raj et al., 2010). Major factors influencing the intra-annual variability of the bloom are also not well highlighted in the earlier studies (Raj et al., 2010).

**Aims**

The aims of the project are to investigate if there is inter-annual variability in the onset of the enhanced chlorophyll east of Madagascar and to study the physical mechanisms that control the onset, propagation and termination of the enhanced chlorophyll.

**Objectives**

- Determine what the mean chlorophyll value is for the region where the bloom occurs
- Determine the onset of the enhanced chlorophyll for each year by looking at persistent levels of chlorophyll above the mean level (bloom index)
- Determine the physical conditions at the onset of the bloom (SST, SLA, winds, currents)
- Determine if the Chl-a signature is influenced by the passage of eddies (cyclonic, anti-cyclonic).

# 2. Literature Review

## 2.1 South Western Indian Ocean circulation

In the South Indian Ocean, the presence of the island, Madagascar, presents unique features to the subtropical gyre circulation (Palastanga et al., 2009) and is characterized by its high circulation variability (DiMarco et al., 2002; Quartly and Srokosz, 2004; de Ruijter et al., 2005; Hermes et al., 2007). It blocks the wind-driven circulation between the latitudes 12°S and 25°S. The anticyclonicsubgyre found east of Madagascar is bounded meridionally by the westward flowing South Equatorial Current (SEC) (between 15°S and 20°S) and the eastward flowing South Indian Counter Current (SICC; Palastanga et al., 2007). As a consequence of Madagascar, the SEC bifurcates into the northward flowing North Madagascar Current (NMC) and the southward flowing East Madagascar Current (EMC) upon encountering the eastern Madagascar coast (Figure 1). The NMC follows the northeast coast of Madagascar until it reaches the northern tip of the island. It then flows westward toward the African coast, where it bifurcates and enters the Mozambique Channel (van der Werf et al., 2009). It is believed that these two currents play a crucial role in redistributing mass and heat along the Madagascar coast and farther to the downstream current (Chen et al., 2014).

## 2.2 East Madagascar Current (EMC)

The EMC, a narrow western boundary current with a width of around 120 km and velocities of about 1.1 $ms^{-1}$ (Nauw et al., 2008), transports approximately 35 Sverdrups (Sv) of warm Indian Ocean waters poleward (Swallow et al., 1988; Nauw et al., 2008). Machu et al. (2002) found that the sea surface temperature (SST) inshore of the EMC had lower SST values, related to the localised upwelling and the presence of a cyclonic eddy (de Ruijter et al., 2004). During their cruise, Nauw et al. (2008) found a deep equatorward undercurrent, the

East Madagascar Undercurrent (EMUC) which is 50 to 90 km wide. The EMUC flows at intermediate depths below the EMC and is more pronounced east of the Madagascar Ridge near 1200m depth (Nauw et al., 2008).

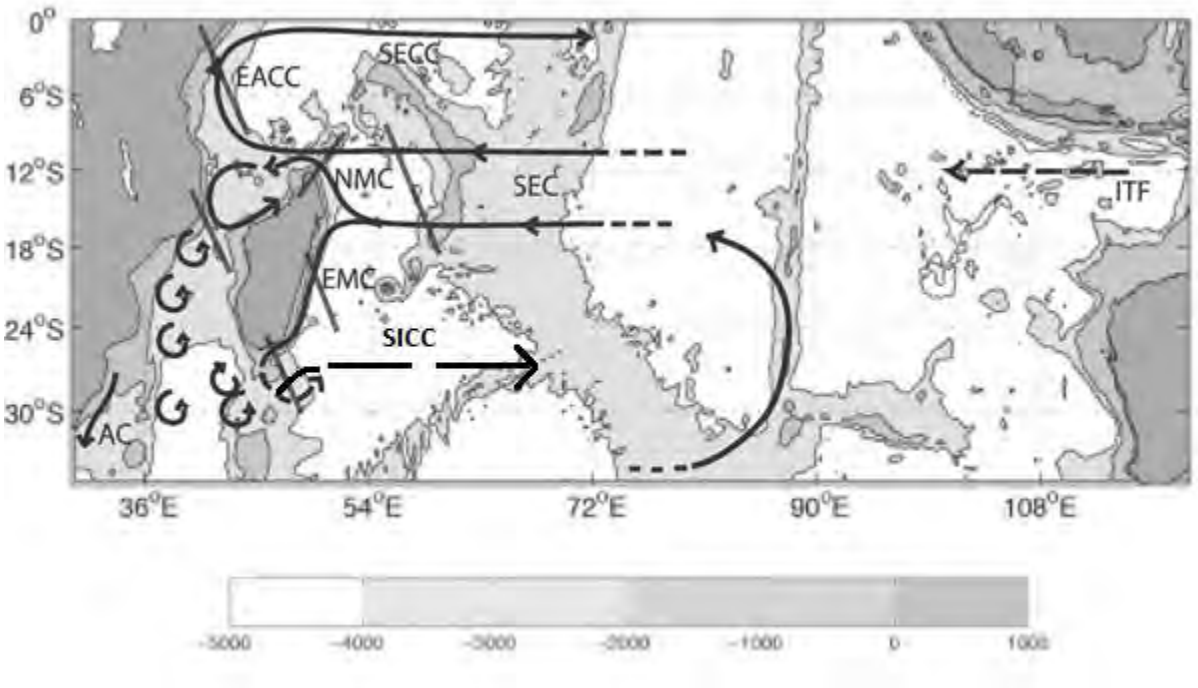


**Figure 1 Schematic of the general circulation of the south Indian Ocean (SIO) and bathymetry (after Palastanga et al., 2006). The tropical gyre in the SIO, formed (only during the summer monsoon season, DJF) from the north of 12°S, consists of the South Equatorial Current (SEC), East African Coastal Current (EACC) and SEC Counter-current (Palastanga et al., 2006).**

The flow path of the EMC is not clear and some hypotheses were suggested. One of them was that the EMC flows due west upon reaching the southernmost part of the island (Grundlingh, 1993; Tomczak and Godfrey, 1994). Lutjeharms et al. (1981) suggested that the EMC retroflects south of Madagascar, with possible shedding of eddies, and flows eastward. During the 2001 Agulhas Current Sources Experiment (ACSEX) hydrographic cruise, de Ruijter et al. (2006) encountered a large counter-rotating vortex pair of eddies southwest of Madagascar, which had a horizontal extent of about 600 km. It had a mature dipolar structure and was deep-reaching (greater than 2000 m). In the anticyclonic lobe, the water mass

characteristics were identical to those of the EMC whereas in the cyclonic one, the water displayed Mozambique Channel (MC) characteristics from the inshore side of the EMC after separation from the current (de Ruijter et al., 2004). This provided the supporting evidence for the suggestion that the cyclonic eddy was formed as a lee eddy at the inshore side of the separating EMC and that the anticyclonic vortex was the result of a retroflection and loop occlusion of the separated EMC jet (de Ruijter et al., 2004).

There is a preferential tendency for cyclonic eddies to be formed directly south and southwest of the Madagascar coast, near the continental shelf while the anticyclonic eddies generally form slightly farther offshore (Halo et al., 2014). The cyclonic and anticyclonic eddies propagate south and westward from Madagascar and many of them reach the Agulhas Current region (Quartly and Srokosz, 2004; Quartly et al., 2006; de Ruijter et al., 2005).

The eddy variability of the EMC has been derived from surface drifters and subsurface floats (Chapman et al., 2003; Shenoi et al., 1999). According to the observations made from satellite altimetry, eddies propagate westward from the east to the EMC (Quartly et al., 2005; de Ruijter et al., 2005). Some of those individual highs and lows which are elongated meridionally are suggestive of Rossby wavefronts, while others are approximately circular which are expected for vortical eddies (Nauw et al., 2008). The variability extends eastward in a latitude band around 25°S and is related to baroclinic instability of the South Indian Counter Current (SICC; Palastanga et al., 2007).

Ridderinkhof et al. (2013) have shown that the EMC breaks up in a series of nearly symmetric dipolar vortex pairs. The frequency of these vortex pairs occurs at about 4 to 6 per year and most of them interact with previously formed cyclonic and anticyclonic eddies after their formation. The dynamics of the evolution of the dipole is dominantly nonlinear due to the large velocity shear across the EMC (Ridderinkhof et al., 2013). Consequently, the EMC

does not retroflect nor does it continue as an unstable westward jet (Ridderinkhof et al., 2013).

Variation in the strength of the EMC is related to the formation of the dipoles (Ridderinkhof et al., 2013). de Ruijter et al. (2004) found that the strength of the EMC varies at inter-annual time scales which is related to climatic modes. This may explain the inter-annual variability in Madagascar dipole formation (de Ruijter et al., 2004). The westward propagation across the Indian Ocean of the large scale circulation anomalies associated with the El Niño Southern Oscillation/Indian Ocean Dipole-cycle leads to a lagged response in the strength of the EMC and the associated enhanced or reduced dipole formation as it takes a period of approximately a year (Webster et al., 1999; Murtugudde et al., 2000; Xie et al., 2002; de Ruijter et al., 2004) to cross the basin. During a La Niña event, there would be a strengthening of the EMC and a more frequent occurrence of the Madagascar dipoles and the opposite would occur during an El Niño event (de Ruijter et al., 2004).

The EMC is of particular interest as it is one of the sources of the Agulhas Current and its possible role in the shedding of rings at the Agulhas retroflection by the propagation of eddies (Ridderinkhof et al., 2013) and the associated leakage of Indian Ocean waters into the Atlantic Ocean (Beal et al., 2011). Eddies found south of Madagascar have been tracked with altimetry propagating (south) westward towards the Agulhas Current (Gründlingh, 1995; Schouten et al., 2002), where they may have an impact on the shedding of Agulhas Rings (Schouten et al., 2002) due to the generation of meanders, known as Natal pulses.

## 2.3 South Indian Ocean Counter Current

The subtropical SICC is a narrow eastward current located between 22°S and 26°S and is guided within the westward propagating Rossby wave structure (Siedler et al., 2006; Palastanga et al., 2007). Siedler et al. (2006) identified the SICC as a strong and well-defined current between the region of the southern tip of Madagascar, where it spreads and becomes weaker at about 80°E until it is well-established again between 90°E and 100°E. A recent study done by Menezes et al. (2014) found that the SICC branches as three main jets, namely the southern, central and northern jet, with the southern branch (around 26°S) being the strongest one. The width of the eastward flow is between about 100 and 200 km with speeds greater than 0.5 m/s. Depending on the phase of the planetary waves, a weaker flow can be observed (Siedler et al., 2006). The core of the SICC is around 25°S with surface velocities up to 0.06 m/s and is confined to the upper 250 m at 20°S to 35°S (Palastanga et al., 2007).

With its relatively large eastward transport of 10 Sv and a core of the zonal counter-current which extends to about 800 m, the SICC is an important component of the near-surface subtropical circulation in the South Indian Ocean (Siedler et al., 2006). This transport and extent are similar to the subtropical counter-current in the North Atlantic where the volume of water transported was about 10 Sv (Schmitz, 1996), with an eastward flow at 700 m (Rossby et al., 1983). However, in the Pacific the current cores were found at shallower depths, above about 250 m (Qiu, 1999; Qiu and Chen, 2004). In the central parts of the subtropical South Indian Ocean, baroclinic instability can be expected to play a role in the ocean dynamics (Siedler et al., 2006). Distributions of potential vorticity at about 250 m and 500 m (McCarthy and Talley, 1999) show a change of sign in the region to the north, between the SICC and the SEC which corresponds to the necessary condition for baroclinic instability

(Kantha and Clayson, 2000; Palastanga et al., 2007) which explain the observed eddy variability in the latitude band of 25°S (Palastanga et al., 2007).

## 2.4 Phytoplankton bloom

The Madagascar plankton bloom is one of the largest dendroid blooms in the world oceans. It develops in austral summer, at 25°S, south east of Madagascar, in a zonal direction, reaching from the coast of Madagascar at 47°E up to 70°E into the South Indian Ocean (Huhn et al, 2012). Longhurst (2001) was the first to report the seasonal development of the dendritic phytoplankton bloom occurring east of Madagascar in the late austral summer. The largest extent of the bloom is reached in February or March in most years, but a strong inter-annual variability exists (Huhn et al, 2012). In April, it becomes very diffuse and is in regression, thus the oligotrophic regime is restored in May of each year as the bloom dissipates (Longhurst, 2001).

The surface bloom is confined to the shallow (~30 m) mixed layer as seen in the SeaWiFS data (Srokosz and Quartly, 2013). The eastward propagation of the bloom and its confinement within a narrow zonal band with low chlorophyll values in adjacent regions, can be associated to the presence of zonal jets in SICC (Huhn et al., 2012). Huhn et al. (2012) suggested two basic mechanisms for the impact of the SICC on the bloom based on geostrophic velocities derived from altimetry data and the use of Lagrangian methods. Firstly, the SICC provides a fast and persistent eastward transport and, secondly, its zonal jet-like Lagrangian Coherent Structures acts as a transport meridional barrier, thus shaping the boundary of the bloom.

Poulton et al. (2009) found that the bloom is mainly composed of nitrogen-fixing cyanobacteria, *Trichodesmium*, which dominate the bloom nearer to Madagascar, while the

diatom, *Rhizosoleniaclevei,* dominates further from the island, in the Madagascar Basin. Analogously, Raj et al. (2010) showed that the diazotroph, *Trichodesmium*, stimulates the bloom and that one of its major sources is from the upwelling occurring along the south coast of Madagascar which provides the necessary nutrients for the bloom formation and the possible factors that may affect the intra-annual and inter-annual variability of the bloom are: upwelling intensity, precipitation, light limitation, mesoscale eddies, EMC and large-scale climate modes such as ENSO. Raj et al. (2010) showed that the upwelling along the coast was likely due to the combined effect of the westward flowing EMC and the zonal component of the wind. There is higher precipitation and photosynthetically available radiance (PAR) during austral summer, leading to favourable conditions (increased stratification and input of nutrients from runoffs) for the development of Cyanobacteria blooms (Raj et al., 2010). The presence of continuous chains of eddies during summer (JFM) in the Madagascar Basin was also shown. The EMC exhibits two different routes during the bloom and non-bloom years, that is, westward and southwestward respectively. These have an effect on the chain of mesoscale eddies and they observed that the bloom was absent after every El Niño event.

There are various hypotheses that were suggested for the possible mechanism that causes the bloom. Longhurst (2001) classified it as an 'entrainment bloom' whereby cold, nutrient-rich water from the mixed layer depth (MLD) is shoaled, resulting from upwelling at the core and the periphery of the cyclonic and anti-cyclonic eddies respectively. Srokosz et al. (2004) described it as a plankton wave originating near Madagascar which travels from west to east, against the mean flow (Rossby wave and eddy propagation direction) and where its meridional extent is limited to a region of high eddy variability (~22°S to 28°S). Uz (2007) proposed that the bloom occurred within a shallow MLD and was caused by diazotrophic nitrogen fixation instead of the entrainment of nutrients. Iron is needed for nitrogen fixation

and Uz (2007) hypothesized that bloom development is stimulated by iron input from river sources which alleviates the iron limitation of diazotrophs. However, the main rivers on Madagascar drain to the west and therefore iron deposition from run-off is highly unlikely to contribute to the waters in the EMC (Srokosz and Quartly, 2013). In addition, the concentration of aeolian iron deposition is too small to have a significant impact on the phytoplankton growth (Mahowald et al., 2009) and would be highly unlikely due to the prevailing easterlies that would blow the dust particles in the westward direction (Srokosz et al., 2004). A more likely source of iron would be from the sediments on the continental shelf south of the island. But, as the bloom is intermittent inter-annually, the release of iron should also vary inter-annually and there is no data available to confirm the hypothesis of the bio-availability of iron (Srokosz and Quartly, 2013).

## 2.5 Climate Variability

### 2.5.1 El Niño Southern Oscillation (ENSO)

The El Niño Southern Oscillation (ENSO) is a naturally occurring large scale coupled ocean-atmospheric mode that affects the inter-annual climatic variability on a global scale. Over the past 50 years, ENSO has frequently occurred throughout a period of global warming (Nicholls, 2008). It is a unique phenomenon in terms of its strength, predictability and global influence. It affects the worldwide weather patterns variability through atmospheric teleconnections (McPhaden et al, 2006). ENSO involves the oscillation between warm and cold conditions in the sea surface temperatures and atmospheric pressure in the equatorial Pacific. It consists of three phases: the warming phase (El Niño), the cooling phase (La Niña) and the neutral phase. El Niño and La Niña typically occur every 2 to 7 years. These events develop in association with swings in the Southern Oscillation which is an atmospheric

pressure pattern, spanning the tropical Indian and Pacific Oceans that is closely related to the strength of the Pacific trade winds (McPhaden et al, 2006).

ENSO cycles are widely studied as they influence the climate worldwide due to changes in the atmosphere in the equatorial Pacific that alter the global atmospheric circulation (Chen and Cane, 2008). The combination of the first and second basic elements of the ENSO cycle, the Bjerknes and equatorial wave feedbacks, controls the degree and duration of individual ENSO events and the interval between them (McPhaden et al, 2006).

Under normal conditions, strong trade winds blow from east to west across the Pacific Ocean, (high to low), the air rises and a low pressure system develops. Moist air rises and evaporation occurs. The air mass begins to cool as it rises (adiabatic cooling) and as a result rainfall occurs. A Walker circulation cell (convection pattern) is formed. In the high pressure system, warm dry air descends near South America (adiabatic heating). Cold water is upwelled along the coast of South America due to the water blown across the equator. Warm water accumulates in the western pacific. La Niña can be considered as the intensification of the normal conditions (Figure 2). The resulting east-west surface temperature contrast reinforces an east-west air pressure difference across the basin that in turn drives the trades (McPhaden et al, 2006). During an El Niño, a high pressure system and low pressure system is formed in the western and eastern Pacific, respectively. Adiabatic heating occurs in the western Pacific and adiabatic cooling occurs in the eastern Pacific. The trade winds weaken and break down which prevents the warm water from propagating westward. The accumulation of warm water in the eastern Pacific prevents upwelling from occurring.

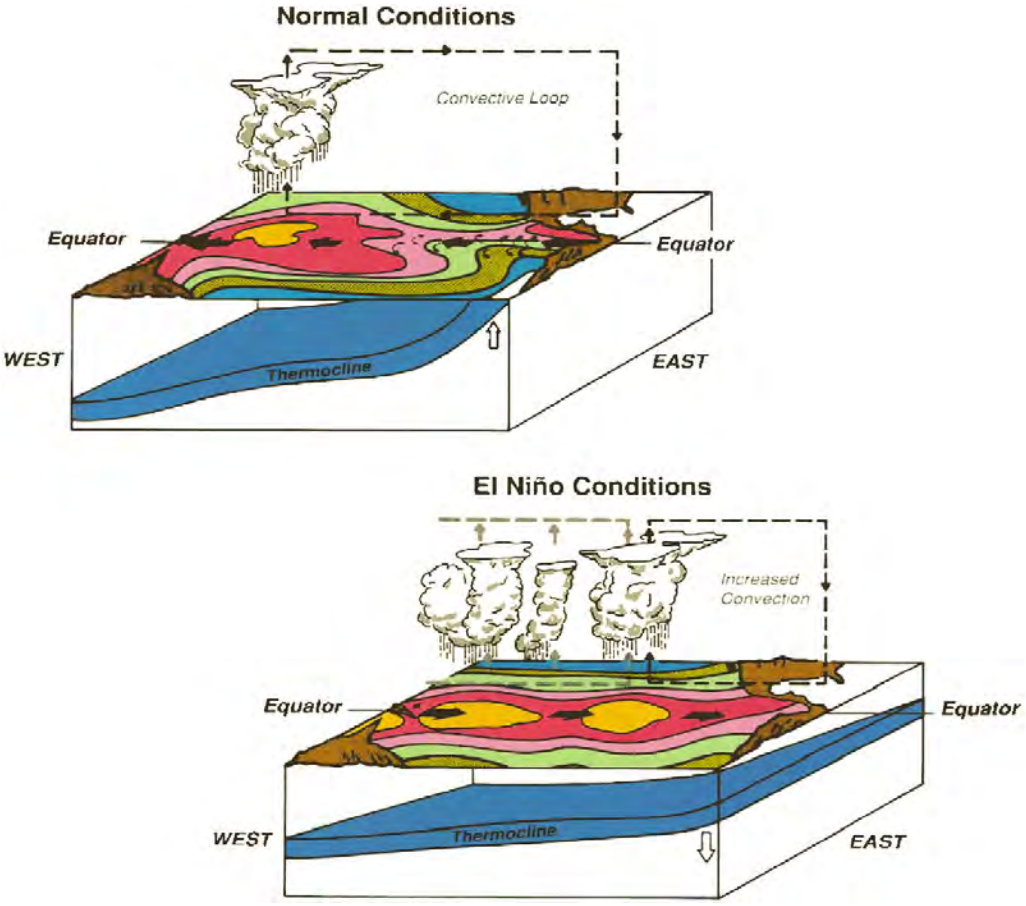


**Figure 2 Schematics of Normal Conditions and El Niño Conditions in the equatorial Pacific Ocean and atmosphere to illustrate the Bjerknes feedback (Cane, 2005).**

The two common indices used to asses ENSO are the NIÑO3.4 and the Southern Oscillation Index (SOI). NIÑO3.4 index is one of the ENSO indicators based on the sea surface temperature (SST). It is the average SST anomaly across the region 5°N to 5°S, 170°W to 120°W (Figure 3). An El Niño (La Niña) event is identified if the 5-month running-average of the NIÑO3.4 index is greater than a positive (negative) anomaly of 0.5°C (McPhaden et al., 2006). The SOI is the difference in sea level pressures measured from Darwin and Tahiti. It has been found that the quasi-cyclic warming and cooling of the eastern and central Pacific leaves its distinctive fingerprint on sea level pressure, particularly, when the pressure measured at Darwin is compared with that measured at Tahiti, the difference between the two

can be used to generate an "index" number. A positive index indicates a La Niña (or ocean cooling) event, while a negative index indicates an El Niño (or ocean warming) event.

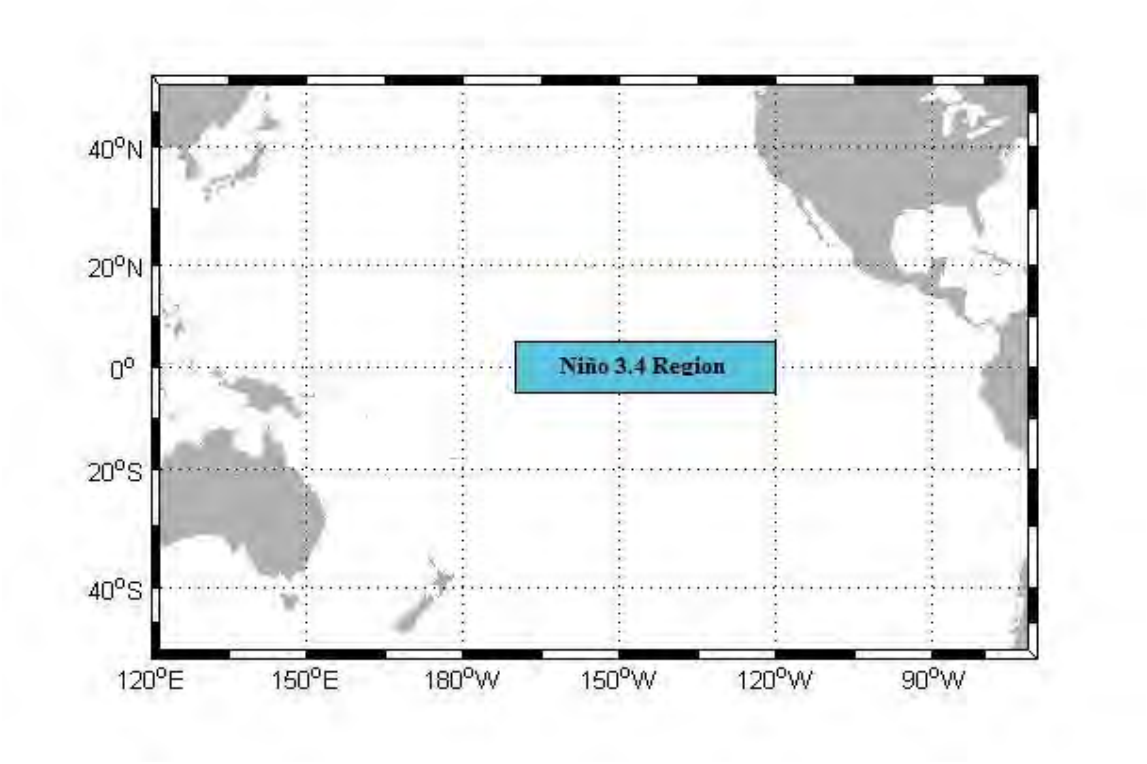


**Figure 3 The shaded region shows the NIÑO3.4 region in the Pacific Ocean from 5°N to 5°S latitude and 120°W to 170°W longitude.**

There is increasing evidence showing that changes in the predictability of ENSO can also be influenced from outside sources, either internal or external to the coupled ocean-atmosphere system even though the basic mechanism of ENSO is contained in the tropical Pacific (Chen and Cane, 2008). Within the tropics, an obvious source of influence is from the Indian Ocean (IO) sector. In the IO, many empirical analyses indicate that the dominant inter-annual variability is closely related to ENSO (Nigam et al., 1993; Tourre and White, 1995; Nicholson, 1997; Yu and Rienecker, 1999; Reason et al., 2000) with the warm water pool that straddles across the western Pacific Ocean and into the eastern IO (Chen and Cane, 2008). It is therefore natural to assume that the climate variations in these two basins are

somehow linked (Chen and Cane, 2008). Regarding the SWIO region, a recent study done by Ridderinkhof et al. (2013), showed that the strength of the southward flowing EMC and the Eddy Kinetic Energy (EKE) occurring southwest of Madagascar appeared to be related to ENSO. The EMC is weaker during an El Niño event and there is also a reduced EKE activity whereas the opposite occurred during a La Niña event (Ridderinkhof et al., 2013)

### 2.5.2 Indian Ocean Dipole

The Indian Ocean Dipole (IOD) is another large scale mode of climate variability in the IO (Saji et al., 1999; Webster et al., 1999). The Dipole Mode Index (DMI) is used to identify the phase of the IOD. It is the difference between the anomalies of sea surface temperature (SST) of the averaged areas of the southeastern (between 0°S to 10°S and 50°E to 70°E) and western (between 10°S to 10°N and 90°E to 110°E) IO. A positive (negative) IOD is characterized by cooler (warmer) SST anomalies in the southeast and warmer (colder) SST anomalies in the west. During IOD events, SST anomalies are strongly coupled to surface wind anomalies in the central equatorial Indian Ocean (Saji et al. 1999, Saji& Yamagata 2003). A positive and negative IOD is when the normalized standard deviation of the DMI is greater than one and lasts for a period of three to four months (Martin and Shaji, 2014).

During the peak phase of a positive IOD event, a reversal of the surface wind direction, from westerlies to easterlies, is caused (Rao et al. 2002). The wind anomalies also strongly influence sea level (Rao et al. 2002) and thermocline anomalies (Feng& Meyers 2003). The sea level anomalies are lower in the east and higher in the central and western IO during positive IOD events (Saji and Yamagata, 2003). The anomalous thermocline has a sign opposing that of sea level (Saji and Yamagata, 2003) according to the theory of a baroclinic response to the wind anomalies in the equatorial regions (McCreary & Anderson 1984).

Palastanga et al. (2006) showed that there is a connection between the mesoscale eddy activity around Madagascar and the IOD from altimetry data. Changes in the intensity and/or position of tropical and subtropical gyres in the South IO could occur according to the IOD phases, which in turn modify the flow east and south of Madagascar (Palastanga et al., 2006). Large-scale sea surface height (SSH) signals propagate as forced Rossby waves and arrive at the coast of Madagascar about 1 year after each IOD phase (Palastanga et al., 2006). Palastanga et al. (2006) found that positive (negative) SSH anomalies associated with a positive (negative) IOD event weaken (intensify) the surface flow of the SEC and its branches, the NMC and EMC.

## 3. Data and Methods

Remote sensing is a useful tool to obtain data for inaccessible and data-poor regions. Due to the lack of in situ data in the study region (Figure 4), the data for the different parameters were obtained from satellites. The study region was divided into two sub-regions, where the bloom has been reported historically, namely, South East region (48°E to 66°E, 24°S to 30°S) and the East region (70°E to 88°E, 24°S to 30°S). These two sub-regions were chosen to allow for the comparison of different areas where the Chl-a concentration vary, low and high. The areas within them were averaged for the time series analysis of the parameters. The anomalies were calculated by doing the climatological mean for each month and the value obtained was subtracted from the monthly values for the selected regions.

A wavelet analysis was performed as it decomposes a signal by estimating its spectral characteristics as a function of time (Torrence& Compo 1998). It reveals how the different scales of the time series change over time as the wavelet function is stretched in time by varying its scale (Daubechies 1992). In this study, the continuous Morlet wavelet transform was used as the wavelet base function as it detects high frequency episodic events (Winder and Cloern, 2010). All the analyses performed were done in the software, MATLAB R2013a. The colour scale used for all the maps of Chl-a was not linear in order to represent the large span of magnitudes of Chl-a in the ocean.

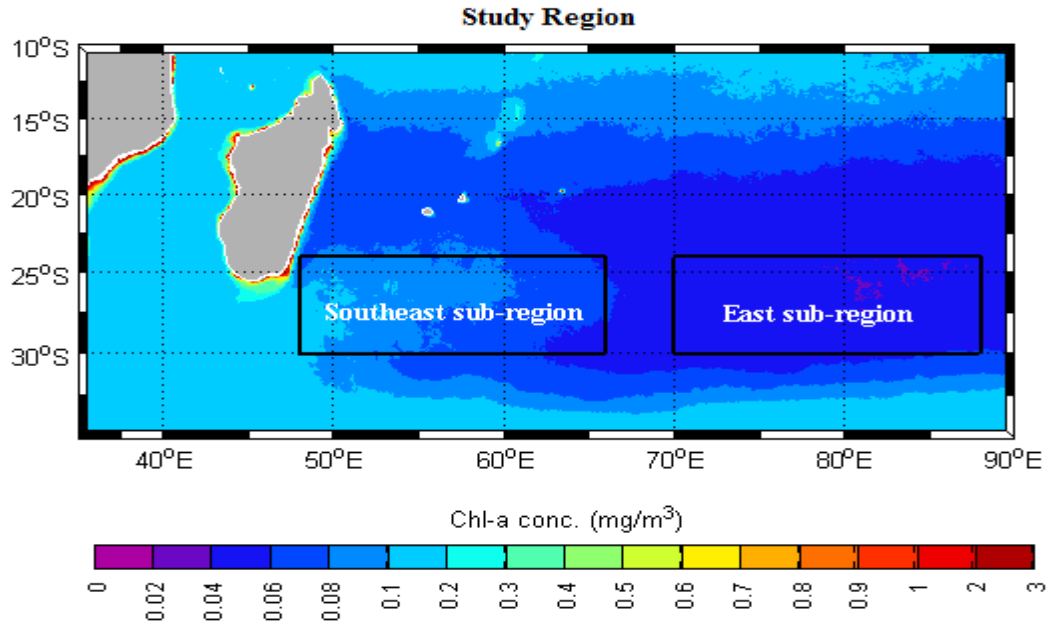


**Figure 4 Map showing the climatological annual chlorophyll concentration (mg/m$^3$) and the study region with the two boxes representing the sub-regions (southeast and east) used for the time series analysis.**

Surface chlorophyll a (Chl-a) and sea surface temperature (SST) data were obtained from the sensor Moderate Resolution Imaging Spectroradiometer (MODIS) on the Aqua satellite. Level 3 data with a spatial resolution of 9 km were downloaded for the 8 day composites, monthly and climatology temporal scales from the Ocean Colour Website (http://oceancolor.gsfc.nasa.gov/) for the period of 2003 to 2013 for both Chl-a and SST.

Sea surface height (SSH) is derived from altimetry measurements. The altimeter, on-board the satellite, emits a radar pulse and measures the time taken for it to travel from the antenna to the sea surface and back to the receiver on the satellite. The SSH is the range from the sea surface to a reference ellipsoid. The data for the sea level anomalies (SLA) were obtained from the Archiving, Validation and Interpretation of Satellite Oceanographic (AVISO) website (http://www.aviso.altimetry.fr/en/) which is the merged product of TOPEX, ERS and Jason-1 altimeters. Maps of SLA (MSLA) obtained from altimeters are used to derive

geostrophic currents. Altimetry data can provide data about how eddies behave in the ocean (eddy size, amplitude, life-time, traveling distance and vorticity, Halo et al., 2014). The data for the SLA and geostrophic currents for the time period of 1992 to 2011 were analysed. The data sets with temporal resolution of weekly, monthly and climatological and a spatial resolution of 0.25° x 0.25° were used.

The SeaWinds scatterometer, on the QuikSCAT satellite, is a microwave radar designed to measure ocean near-surface wind speed and direction. The wind data were acquired from the Physical Oceanography Distributed Active Archive Center (http://podaac.jpl.nasa.gov/) for the time period 2001 to 2009 with a 0.25° x 0.25° spatial resolution for the daily, monthly and climatological temporal resolutions.

The Niño 3.4 index monthly data were obtained from the Climate Prediction Center of National Oceanic and Atmospheric Administration (NOAA) and the Dipole Mode Index (DMI) was acquired from the KNMI Climate Explorer website (http://climexp.knmi.nl/) for the time period 2000 to 2014.

# 4. Results

## 4.1 Spatial distribution of the phytoplankton bloom

The seasonal climatology of the Chl-a concentration, for the period 2003 to 2013, (Figure 5) shows the overall spatial distribution of the Chl-a concentration in the South western Indian Ocean (SWIO) region. There is a high concentration along the eastern coast of Africa and the western coast of Madagascar. The enhanced chlorophyll concentration occurring east of Madagascar can cover a large area, extending to the eastern IO (~70°E) during late austral summer (DJF; Figure 5a) and austral autumn (MAM; figure 5b). During austral winter (JJA; Figure 5c) the bloom occupies most of the region and dissipates during austral spring (SON; Figure 5d). There is also a high level of Chl-a which is apparent in the Mozambique Basin and Mozambique Channel. The bloom is evident in the climatology as it is so strong that it bias's the overall mean.

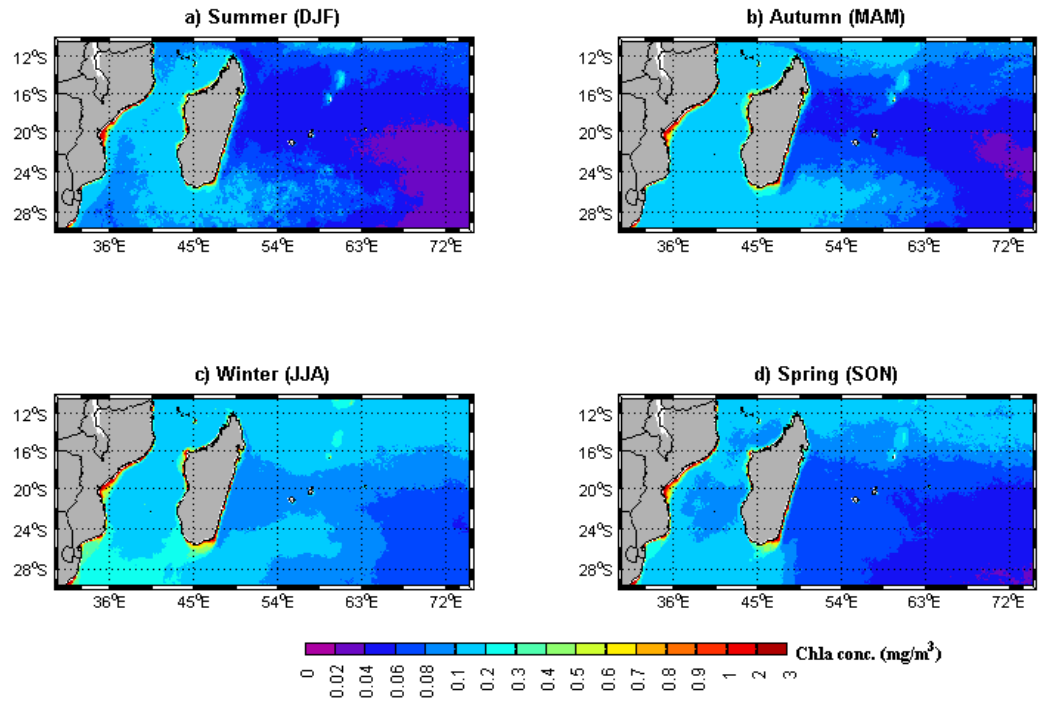


**Figure 5 Climatology of Chl-a concentration (mg/m$^3$) from MODIS for DJF (a), MAM (b), JJA (c) and SON (d).**

## 4.2 Seasonal variation of the satellite datasets

The monthly averaged time series shows how the concentration of Chl-a varies during the period of 2003 to 2013 for the two sub-regions (Figure 6a). The peak in Chl-a between the two boxes is not in phase. In the Southeast box, the seasonality of Chl-a concentration can be seen in the time series, with a maximum during austral winter and minimum in austral summer (2005 and 2011). During 2006, 2008, 2009, 2012 and 2013, there was a semi-annual signal, transposed onto the annual signal, with a peak in late austral summer (the bloom) and in austral winter (the average maximum) with a Chl-a concentration higher in summer than in winter. In some years (2003, 2005, 2007 and 2010), the semi-annual signal was not evident and the seasonal signal corresponding to the increase of Chl-a concentration in austral winter dominated, with no summer peak (i.e. the bloom). The large Chl-a concentration which can occur during some years in the Southeast box during austral summer does not translate into large values in the Eastern box. In the Eastern sub-region (70°E to 88°E, 24°S to 30°S, hereafter referred to as East box), the Chl-a concentration demonstrates an annual cycle, with only the peak during winter which is expected as the bloom does not reach this far east. The anomalous peaks in the annual cycle of the Eastern box tend to occur during a non-bloom year in the Southeast box (2003, 2005 and 2007). During 2010 and 2011 there was anomalously low Chl-a in boxes.

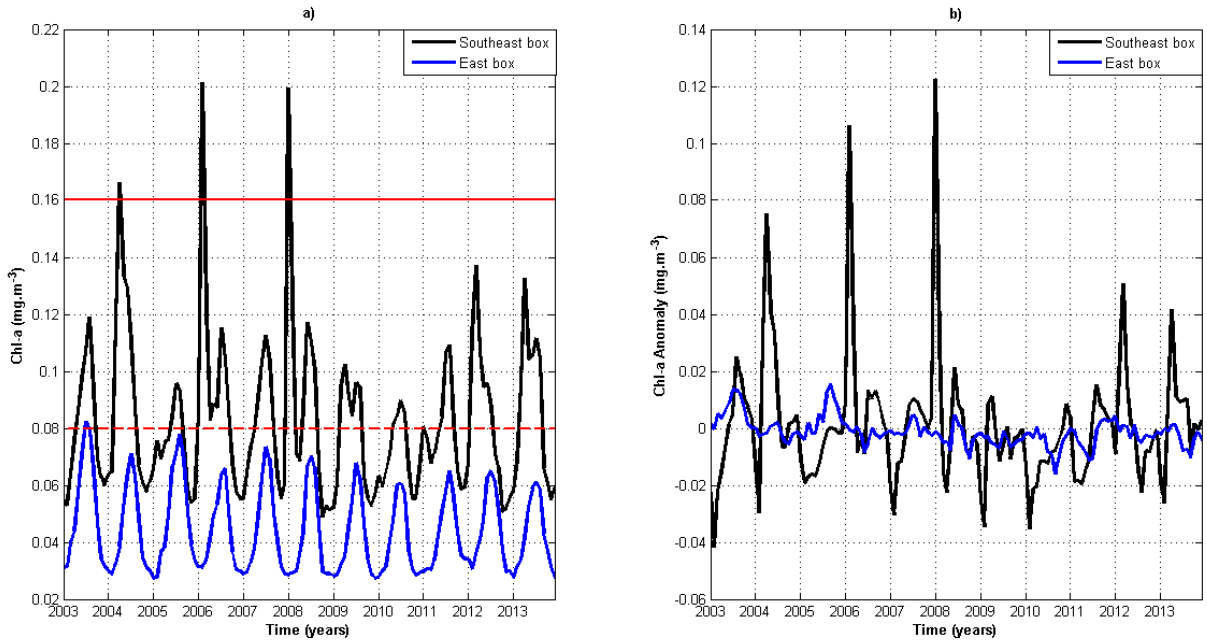


**Figure 6 a) Monthly averaged time series of Chl-a concentration (mg/m$^3$) with the mean level for the Southeast box (dashed line) and threshold value (thick line) for the characterization of a bloom year and b) Chl-a concentration anomaly (mg/m$^3$) for 11 years (2003-2013) of the selected regions.**

The seasonality of SST can be seen in the monthly averaged time series of SST (Figure 7a). There is an increase in temperature (above 24°C) during austral summer and a decrease (below 22°C) during austral winter in the two sub-regions. The SST was lowest (~20.5°C) during the winter of 2003 and highest during the austral summer of 2006 (~27.3°C) for the South East box. In the East box, the highest SST was ~26°C in 2010 (austral summer) and lowest during the austral winter of 2005 (~19.5°C). The SST anomalies of the two sub-regions are not in phase with each other (Figure 7b). This could be due to the ocean/atmospheric dynamics that affect the SST.

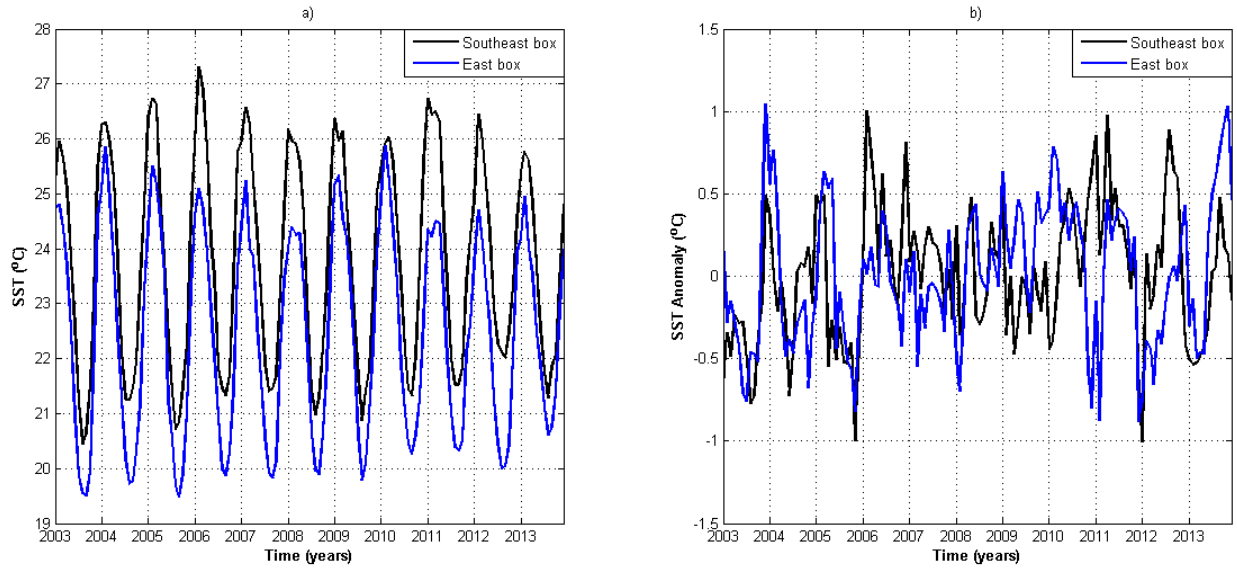


**Figure 7 a) Monthly averaged time series of SST (°C) and b) SST anomaly (°C) for 11 years (2003-2013) of the selected regions.**

Further analysis was performed on the geostrophic currents and wind to investigate the potential causes for the bloom and seasonality. The geostrophic current speed for both sub-regions was stronger during austral spring and summer and weaker during austral autumn and winter (not shown). The wind speed was weaker during austral spring and stronger during austral winter (Figure 8a). The South East box is characterized by a higher eddy kinetic energy (EKE) as compared to the East box, with maxima during austral summer and spring and minima during austral autumn and winter (Figure 19 in Appendix).

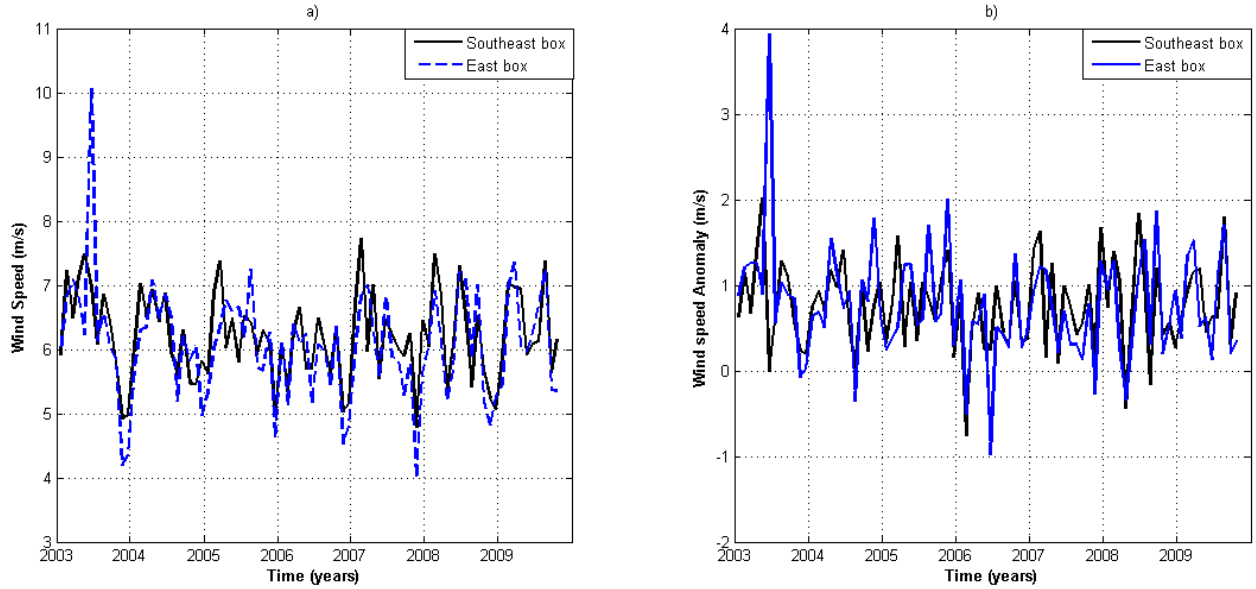


**Figure 8 a) Monthly averaged time series of wind speed (m/s) and b) the wind speed anomaly (m/s) for 7 years (2003-2009) of the selected regions.**

## 4.3 Characterization and identification of bloom

Several authors used different methods to define a bloom as there is no threshold to characterize it. Siegel et al. (2002) and Henson and Thomas (2007) used 5% above the annual median values of Chl-a to define the onset of the blooms whereas Kim et al. (2007) did not define any quantitative threshold but rather, used weekly averaged Chl-a maximum concentrations during the spring and fall seasons as the blooms (Latha et al., 2014). In this study, a bloom is characterized by a Chl-a concentration which is twice the mean level (~0.08mg/$m^3$) of the study region average. Since there is no threshold for the definition of a bloom and the methods are subjective, this threshold was chosen by taking into consideration the low Chl-a values in the study region as opposed to coastal areas where the Chl-a levels are much higher. This method is in accordance with Wilson and Qiu (2008) who characterized a bloom when the concentration of Chl-a is greater than 0.15mg/$m^3$ and where the ambient background level was ~0.08mg/$m^3$. In Figure 6(a), three austral summer blooms

can be seen in 2004, 2006 and 2008 in the South Eastern sub-region. In 2009, 2012 and 2013, the concentration of Chl-a was greater than 0.1mg/$m^3$ but still below the threshold value to be considered as a bloom. The onset of the bloom occurs generally in January, reaches its maximum peak in February and dissipates by the end of March.

Slight variations are visible in the onset, growth and termination periods of the bloom (Table 4.1). In 2004, the bloom was initiated in February, peaked in April (Chl-a concentration of ~0.164mg/$m^3$) and dissipated by the end of April (Figure 9). In 2006, the onset of the bloom was during December of the previous year, peaked in February with a Chl-a concentration of ~0.2mg/$m^3$ and dissipated by the end of March (Figure 10). In 2008, the bloom was initiated in December of 2007, peaked in January instead of February and dissipated by the end of February (Figure 11). The monthly analysis during the specific months of the bloom years shows that the Chl-a concentration can reach above 0.3mg/$m^3$ (March 2004, April 2004, February 2006 and January 2008). The enhanced concentrations of Chl-a for these months are not shown in Figure 6 as it is the average of the selected area which had more regions of lower concentration, leading to a reduced average of Chl-a.

Table 4.1 The year of the bloom and its respective month for the onset, peak and termination of the bloom.

| Year | Onset | Peak | Termination |
|---|---|---|---|
| **2004** | February | April | End of April |
| **2006** | December 2005 | February | End of March |
| **2008** | December 2007 | January | End of February |

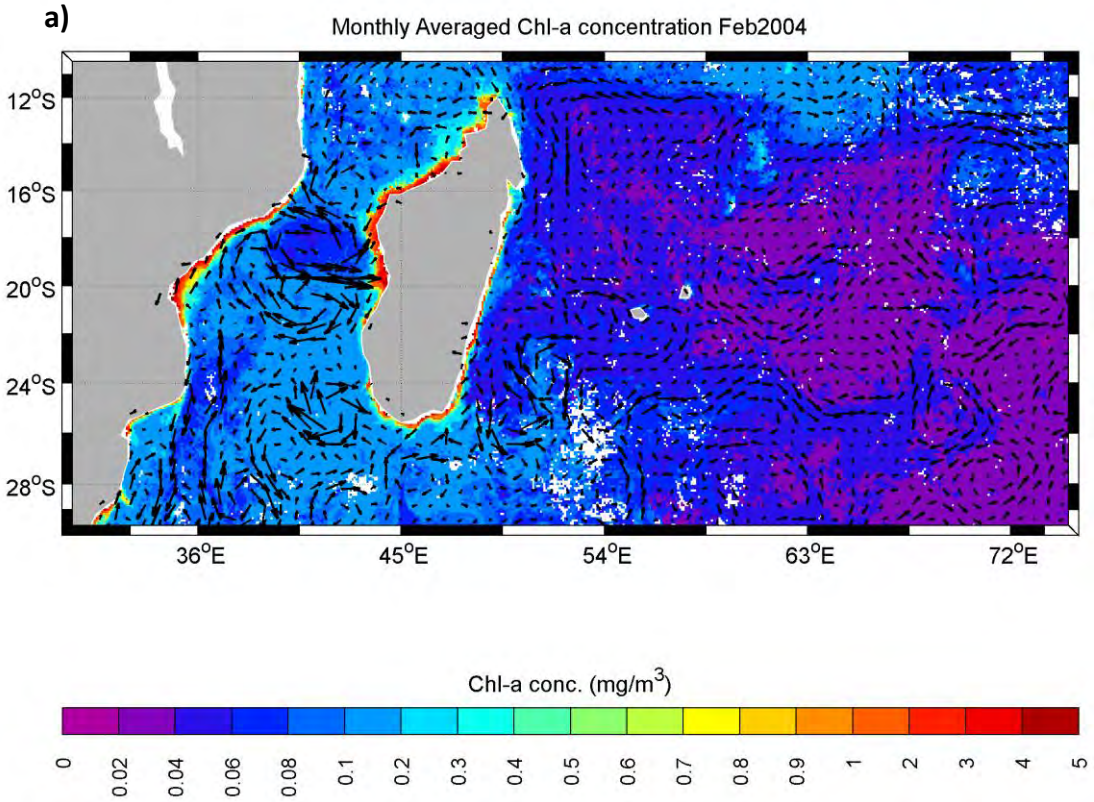
a)
Monthly Averaged Chl-a concentration Feb2004
12°S
16°S
20°S
24°S
28°S
36°E
45°E
54°E
63°E
72°E
Chl-a conc. (mg/m3)
0
0.02
0.04
0.06
0.08
0.1
0.2
0.3
0.4
0.5
0.6
0.7
0.8
0.9
1
2
3
4
5

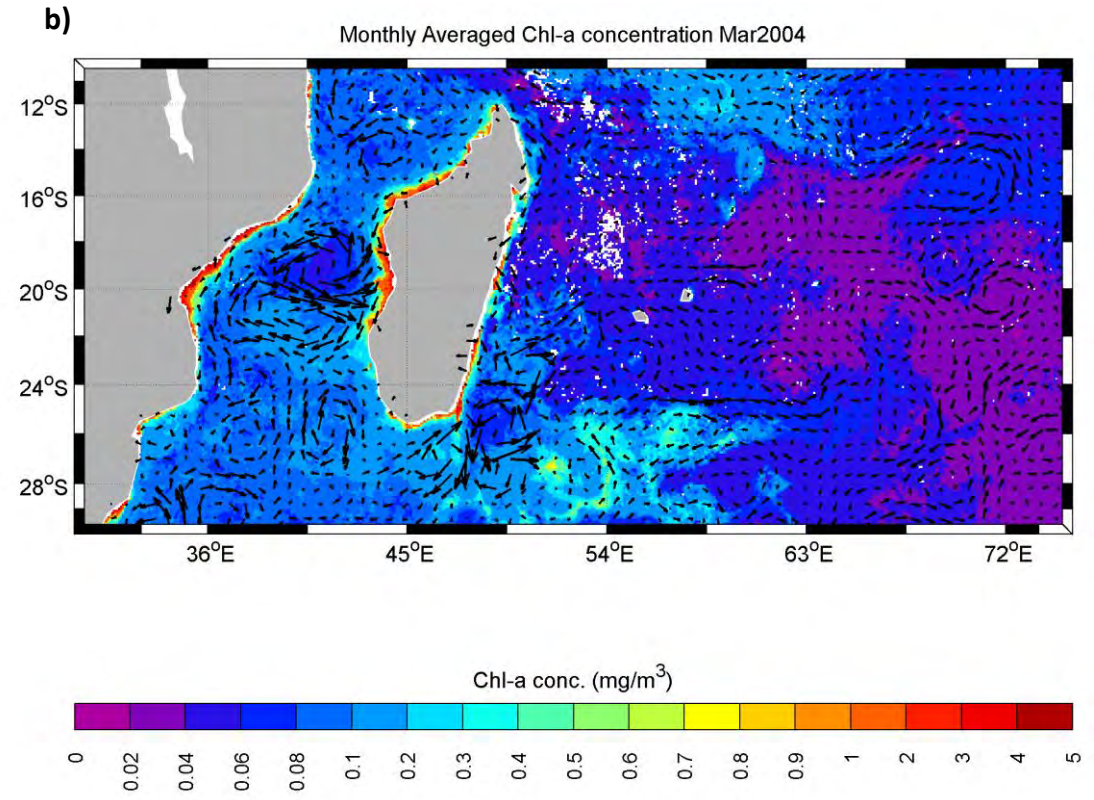
b)
Monthly Averaged Chl-a concentration Mar2004
12°S
16°S
20°S
24°S
28°S
36°E
45°E
54°E
63°E
72°E
Chl-a conc. (mg/m3)
0
0.02
0.04
0.06
0.08
0.1
0.2
0.3
0.4
0.5
0.6
0.7
0.8
0.9
1
2
3
4
5

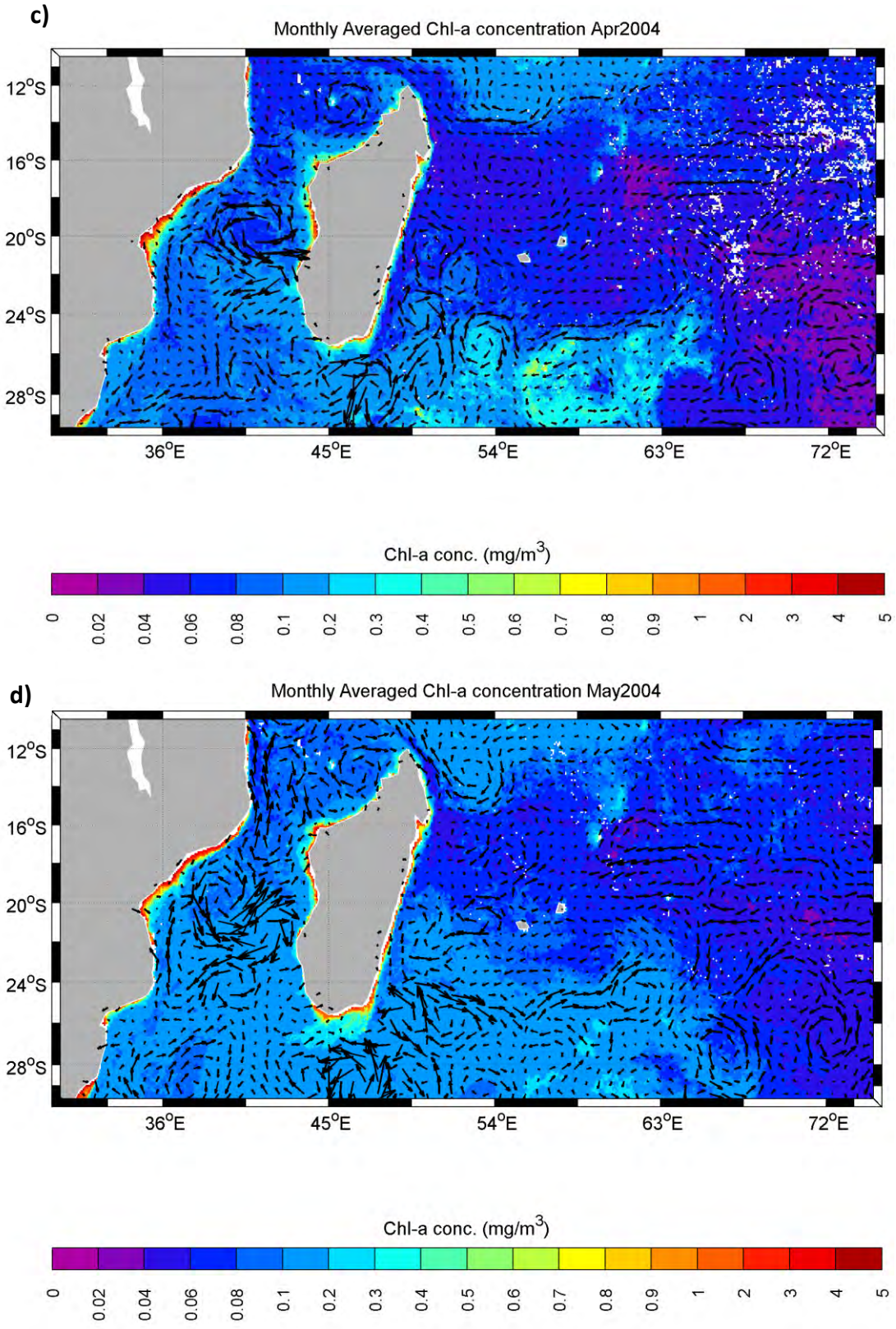


**Figure 9 The monthly averaged Chl-a concentration (mg/m$^3$) and geostrophic currents (m/s) at a) the onset (Feb), b) and c) propagation (Mar and Apr) and d) termination (May) of the bloom during 2004. White patches are the missing data due to cloud cover.**

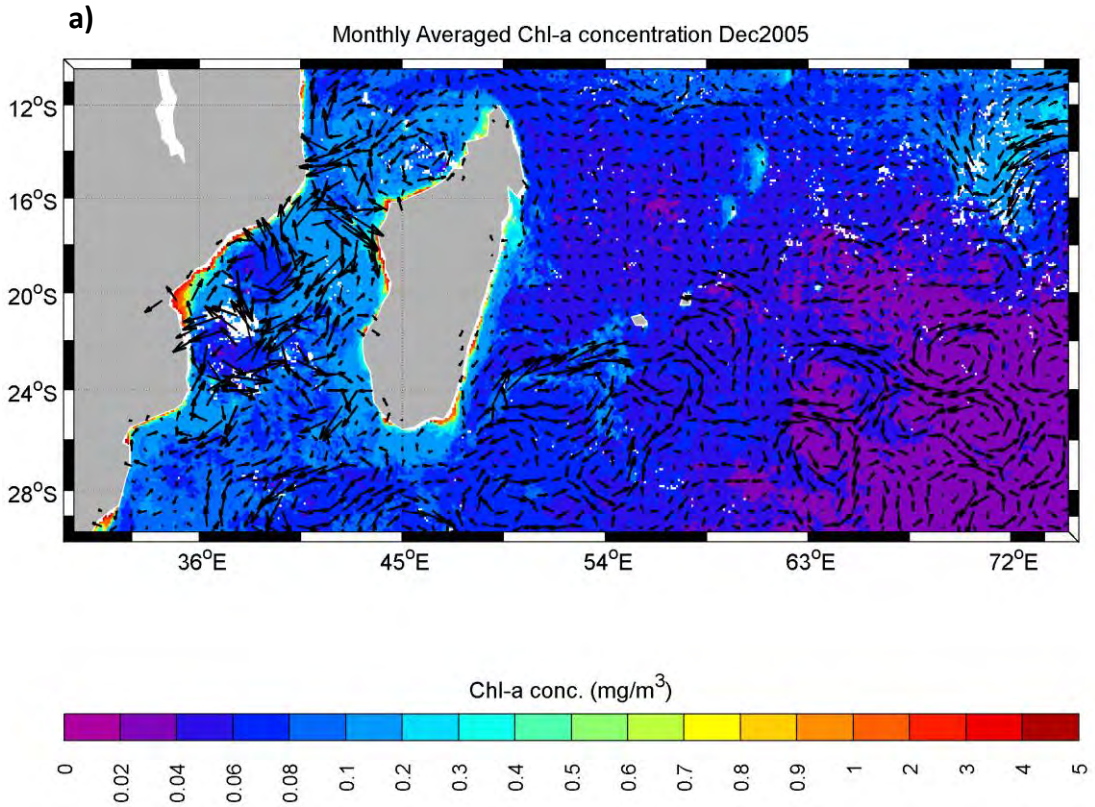
a)
Monthly Averaged Chl-a concentration Dec2005
12°S
16°S
20°S
24°S
28°S
36°E
45°E
54°E
63°E
72°E
Chl-a conc. (mg/m3)
0
0.02
0.04
0.06
0.08
0.1
0.2
0.3
0.4
0.5
0.6
0.7
0.8
0.9
1
2
3
4
5

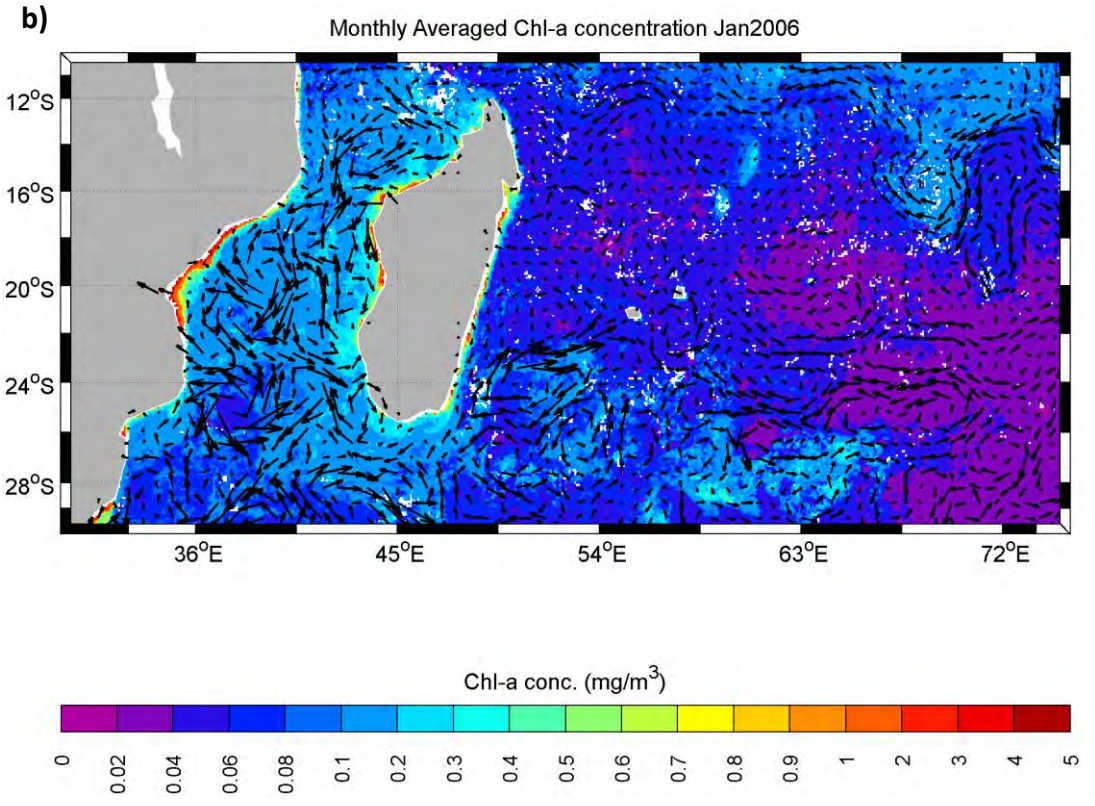
b)
Monthly Averaged Chl-a concentration Jan2006
12°S
16°S
20°S
24°S
28°S
36°E
45°E
54°E
63°E
72°E
Chl-a conc. (mg/m3)
0
0.02
0.04
0.06
0.08
0.1
0.2
0.3
0.4
0.5
0.6
0.7
0.8
0.9
1
2
3
4
5

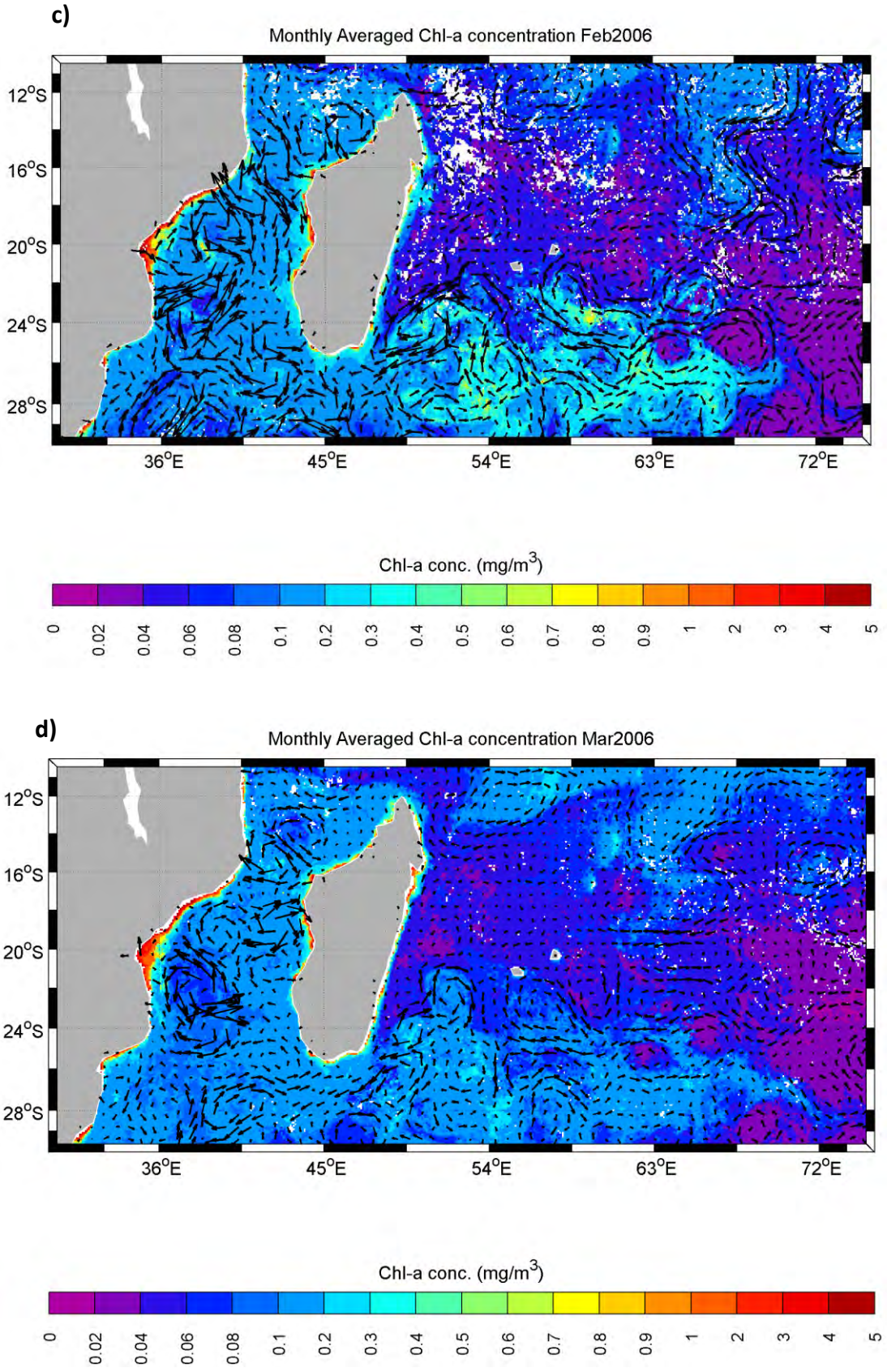


**Figure 10 The monthly averaged Chl-a concentration (mg/m$^3$) and geostrophic currents (m/s) at a) the onset (Dec), b) and c) propagation (Jan and Feb) and d) termination (Mar) of the bloom during 2006. White patches are the missing date due to cloud cover.**

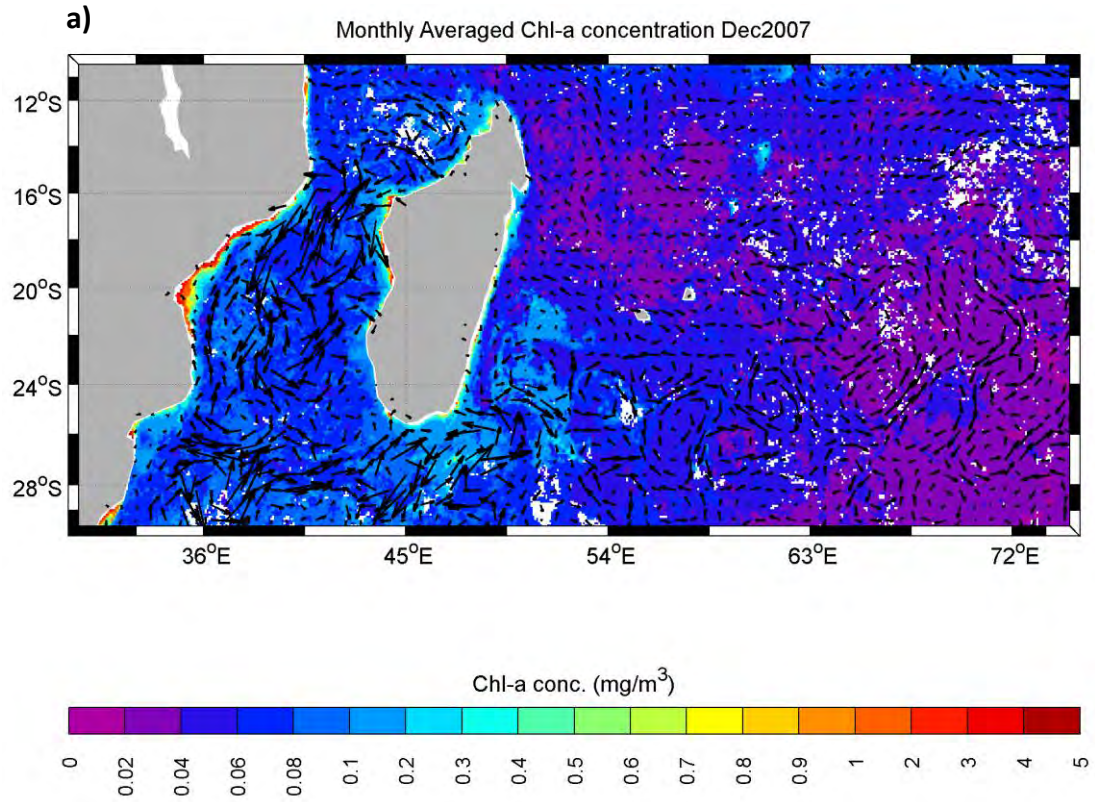
a)
Monthly Averaged Chl-a concentration Dec2007
12°S
16°S
20°S
24°S
28°S
36°E
45°E
54°E
63°E
72°E
Chl-a conc. (mg/m3)
0
0.02
0.04
0.06
0.08
0.1
0.2
0.3
0.4
0.5
0.6
0.7
0.8
0.9
1
2
3
4
5

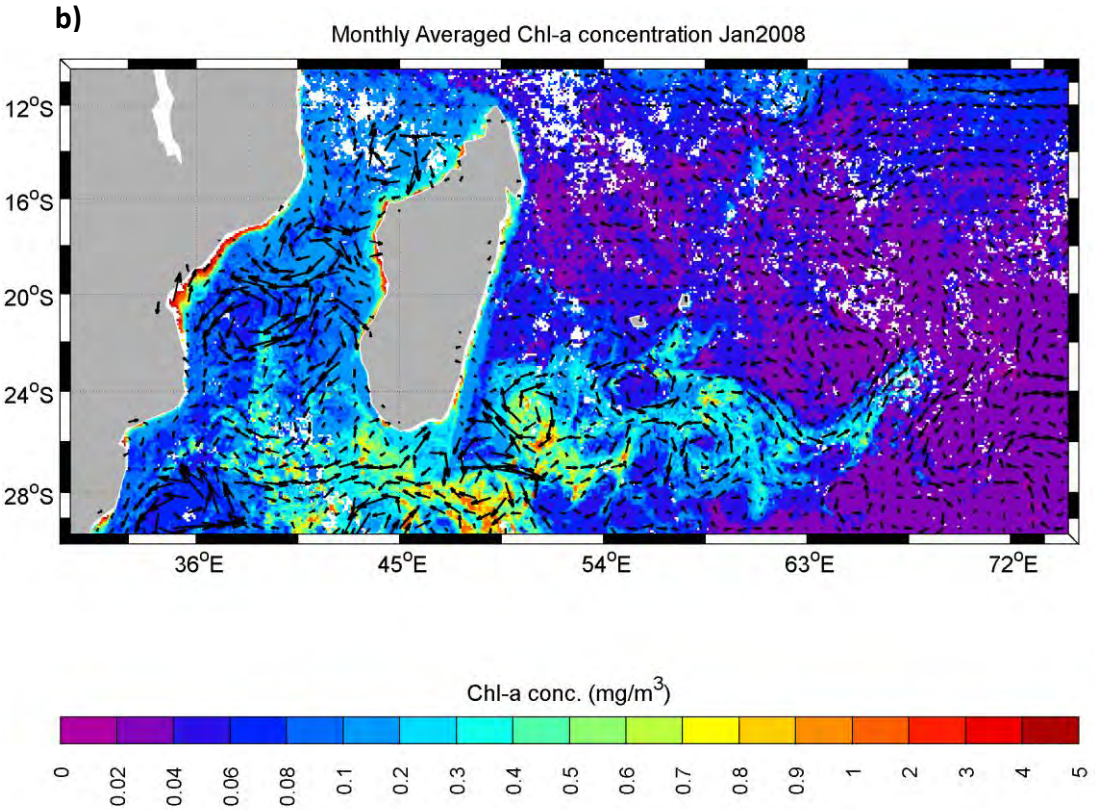
b)
Monthly Averaged Chl-a concentration Jan2008
12°S
16°S
20°S
24°S
28°S
36°E
45°E
54°E
63°E
72°E
Chl-a conc. (mg/m3)
0
0.02
0.04
0.06
0.08
0.1
0.2
0.3
0.4
0.5
0.6
0.7
0.8
0.9
1
2
3
4
5

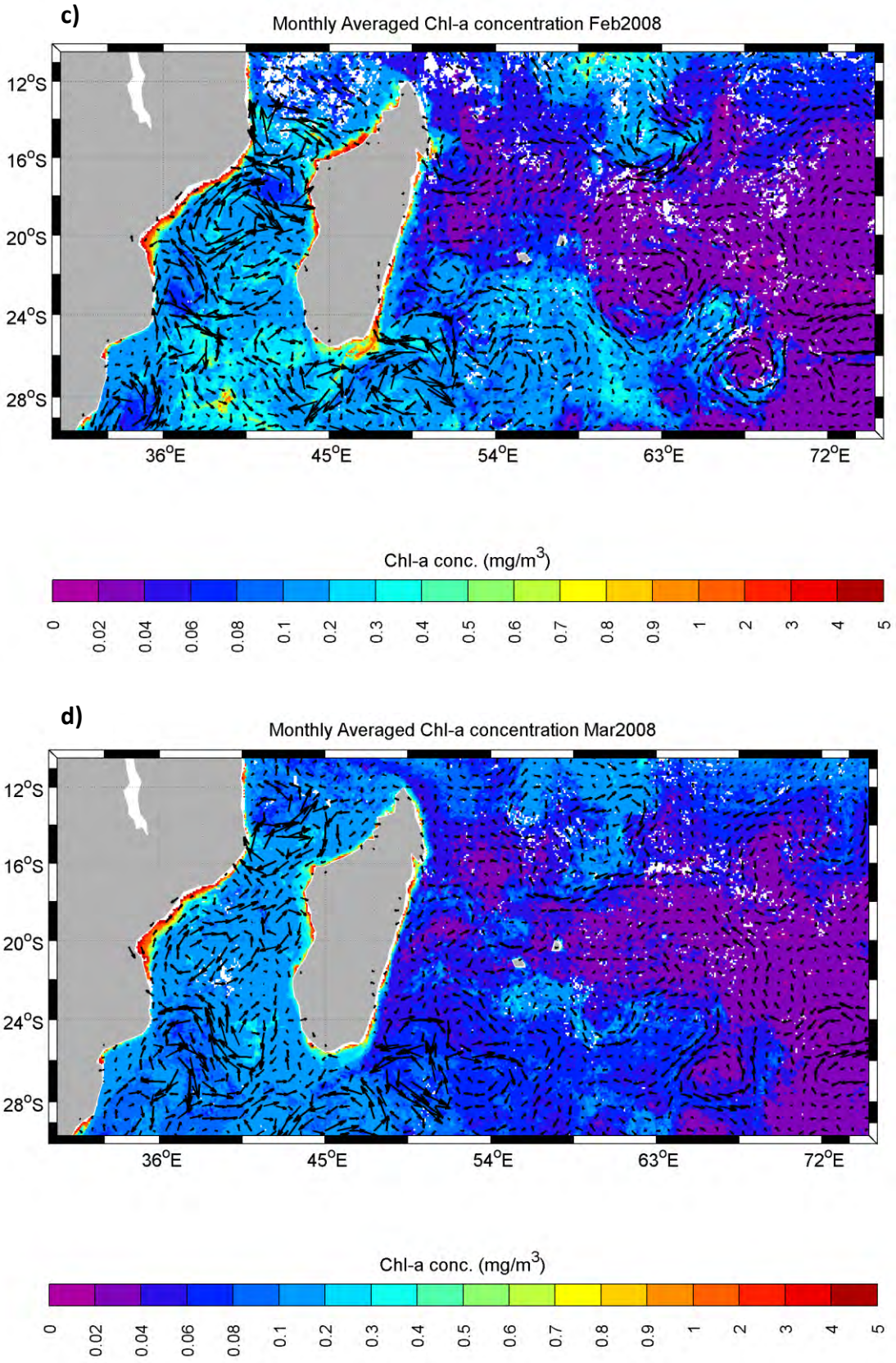


**Figure 11 The monthly averaged Chl-a concentration (mg/m$^3$) and geostrophic currents (m/s) at a) the onset (Dec), b) and c) propagation (Jan and Feb) and d) termination (Mar) of the bloom during 2008. White patches are the missing date due to cloud cover.**

## 4.4 Physical parameters analysed during the bloom years

### 4.4.1 Sea surface temperature (SST)

In order to investigate any relationship between temperature and Chl-a during bloom years (such as upwelling), SST was investigated. A negative SST anomaly, -0.0062°C, -0.4243°C and -0.2580°C was apparent in 2004, 2006 and 2008 respectively (Figure 7b) at the onset of the bloom. The negative anomalies at the onset of the bloom could be attributed to upwelling or entrainment of nutrients but also to rainfall and winds which would decrease the surface temperatures. In order to attribute this decrease to upwelling, the vertical structure of the water column should be analysed to see the doming of the isopycnals.

### 4.4.2 Wind pattern

At the onset of the blooms, the wind speed was between 8 to 10 m/s in February 2004 and was blowing from a southeasterly direction (Figure 12). During December 2005 and 2007, the wind speed was approximately 6 to 8 m/s but the direction was southeasterly and easterly respectively. When the bloom reached its maximum peak, the wind speed was about 6 to 8 m/s and was blowing in an easterly direction. The easterly wind speed at the termination of the bloom was between 7 to 10 m/s for the 3 years.

**a)**

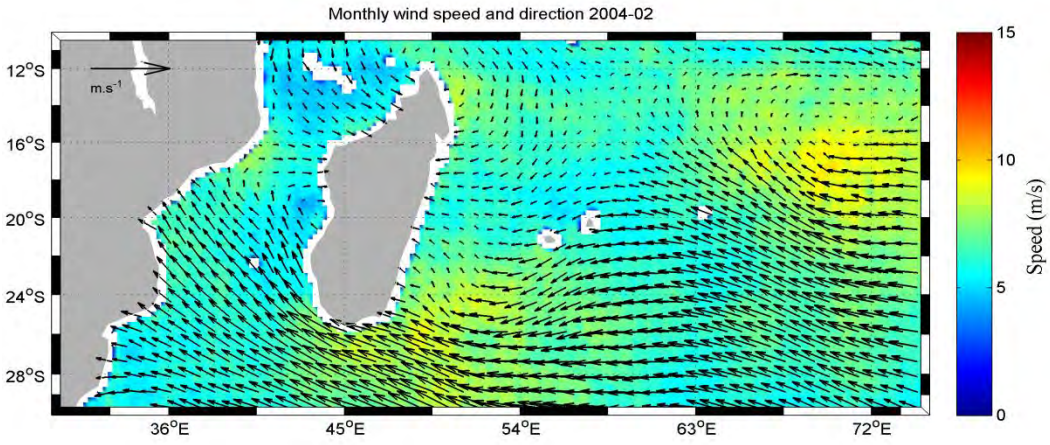

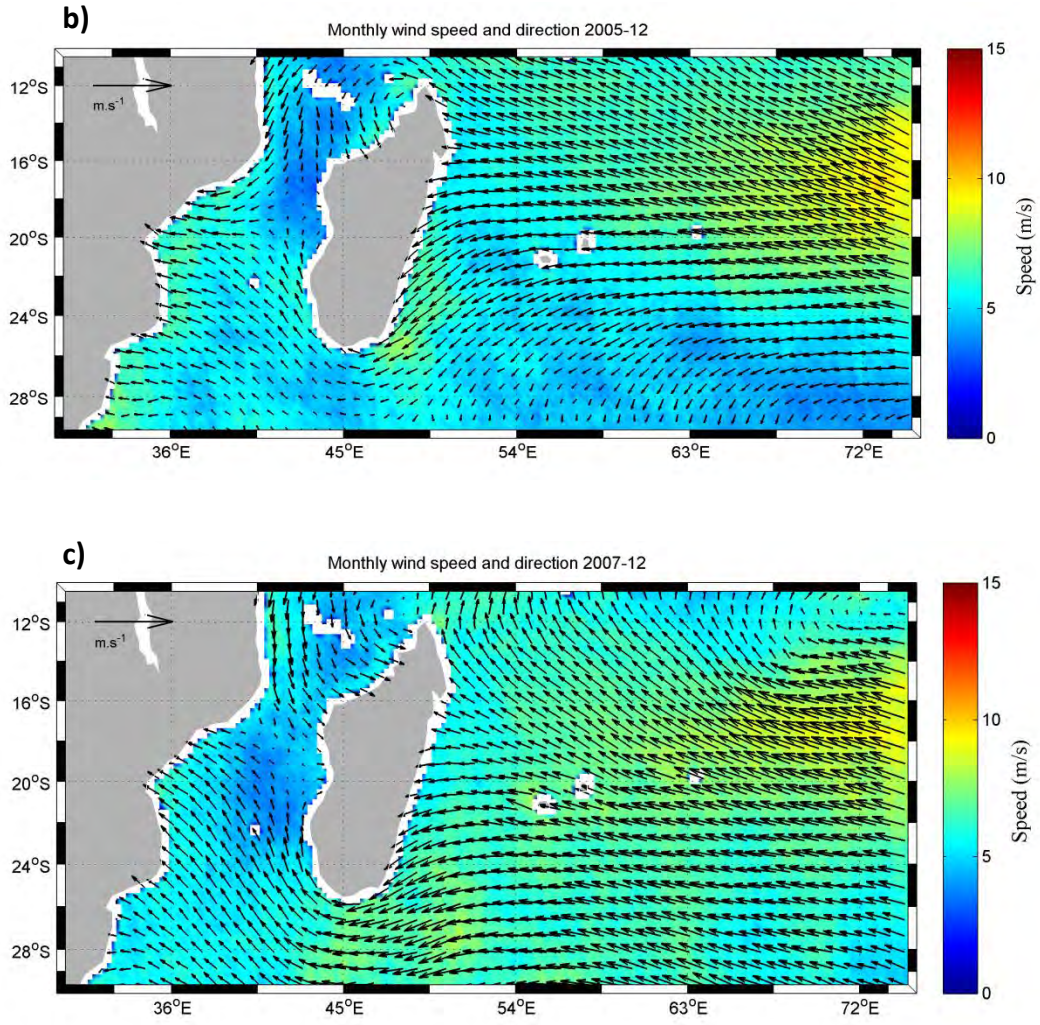


**Figure 12 Wind speed (colour) and direction (arrow) m/s at the onset of the bloom during a) January 2004, b) December 2005 and c) December 2007.**

### 4.4.3 Climate variability

The Niño 3.4 index was used to identify the El Niño and La Niña events. During the period of 2000 until 2014, 6 La Niña and El Niño events occurred with varying intensities (Figure 13). Two El Niño events coincided with the bloom years of 2004 and 2006 and a La Niña event coincided with the bloom in 2008. During 2006 to 2008, there were three consecutive positive IOD (pIOD) events and in 2007, there was a unique occurrence of a pIOD and a La Niña event (Cai et al., 2009).

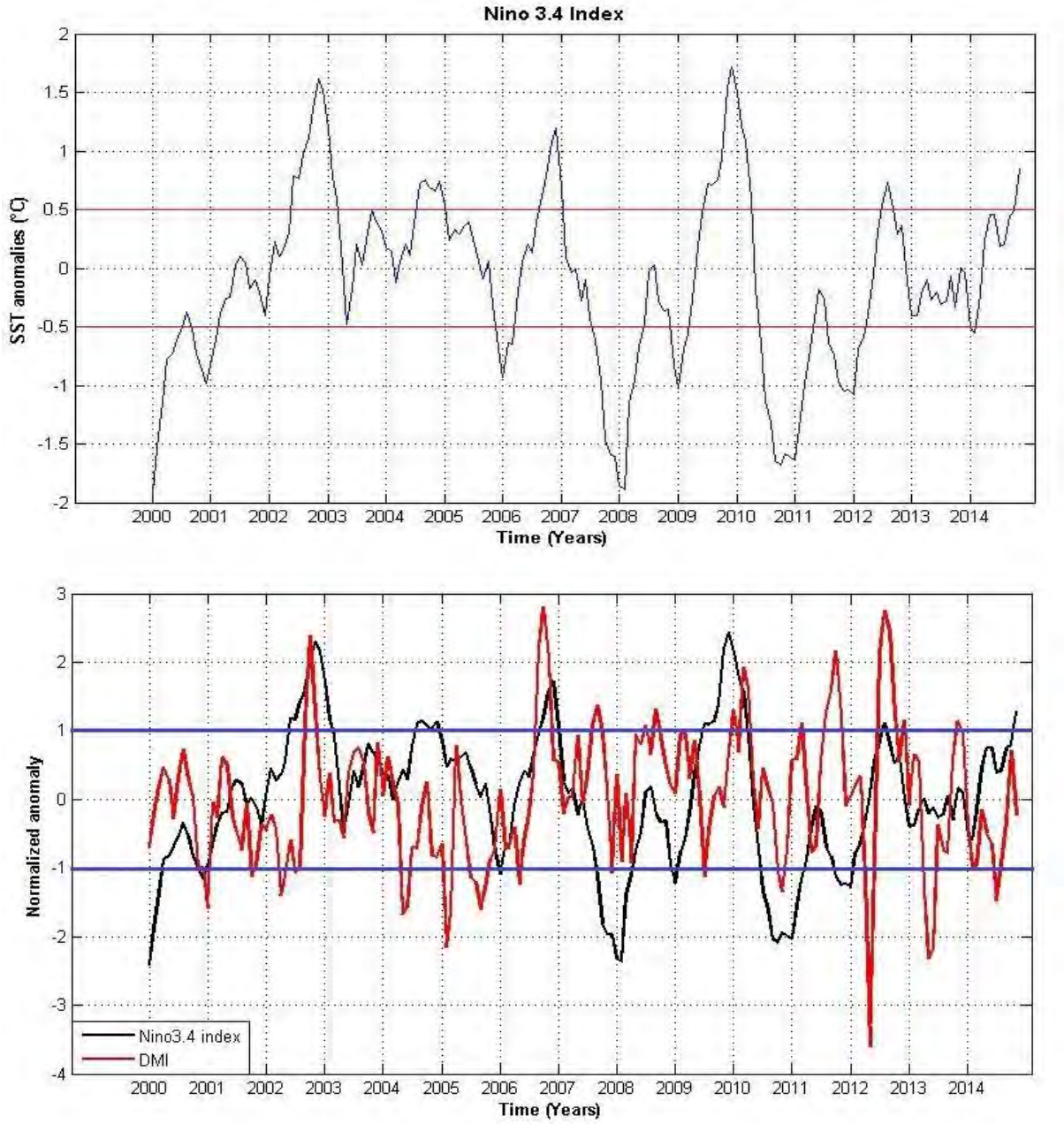


**Figure 13 The monthly Niño 3.4 index (top) for the time period of 2000 to 2014 (the solid red lines at ±0.5 are the threshold values to identify an ENSO event) and the normalized anomaly of the monthly Dipole Mode Index and Niño 3.4 index (bottom) for the time period of 2000 to 2014 (the blue lines at ±1 are the threshold values to identify an IOD event).**

### 4.4.4 Role of eddies in the spatial distribution of the bloom

The longitude-time plots show the SLA during 2004, 2006 and 2008 which were averaged between the latitudes 24°S and 28°S. During these three years, westward propagating eddies

can be seen. In 2004 (Figure 14a), there were approximately 6 cyclonic eddies (negative) that were more prominent than the anticyclonic eddies (positive). In 2006, the anticyclonic eddies dominate. There were approximately 4 cyclonic eddies and 7 anticyclonic ones. The anticyclonic eddies between the longitudes 69°E to 50°E follow a southwest propagation instead of a westward one during the months of June to December (Figure 14b) as compared to 2004 and 2008. In 2008, the anticyclonic eddies were more prominent in the region (Figure 14c). During the non-bloom years, the presence of westward propagating eddies are clearly seen (Figure 17 in Appendix). In 2010 and 2011 (Figure 17e and 17f, respectively), the anti-cyclonic eddies were more intense and prominent than in the other non-bloom years.

The mesoscale eddies play an important role in the entrainment of nutrients in the upper levels of the water column. The nutrients are brought to the surface by their rotary motion. In a cyclonic eddy, cold, nutrient-rich waters are brought to the surface (upwelling) where the Chl-a concentration reaches its peak in the central part. In an anti-cyclonic eddy, the water converges which leads to downwelling, resulting in a decrease of Chl-a concentration. However, high levels of Chl-a concentration can also be seen around the edges of anti-cyclonic eddies (Gaube et al., 2014). Figures 9, 10 and 11 show that Chl-a is advected by the eddies due to their rotary motion.

a)

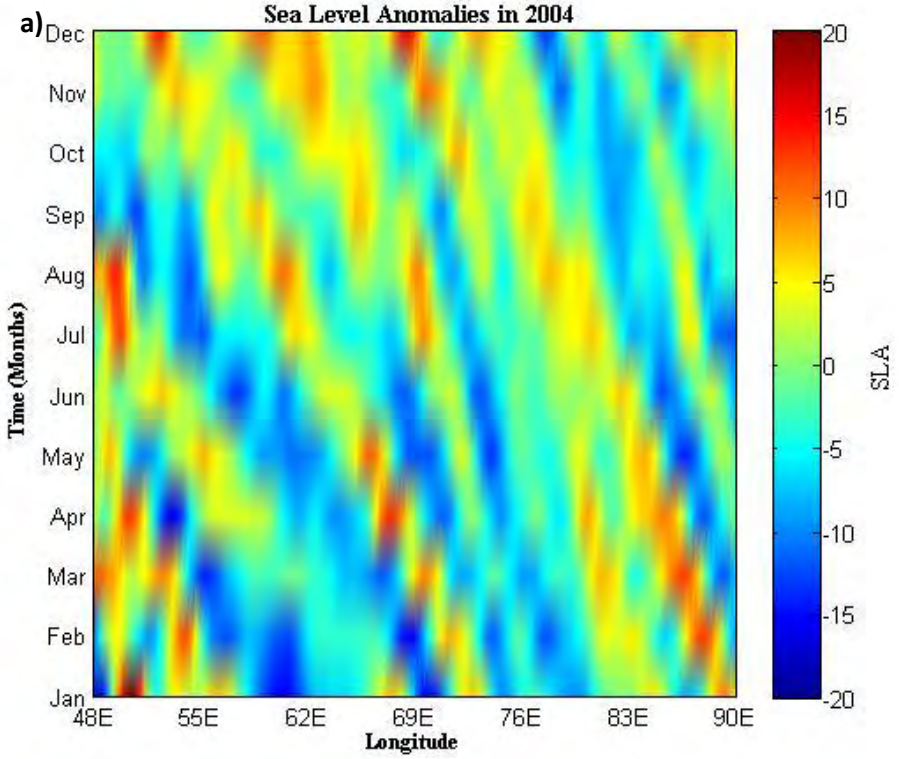
Sea Level Anomalies in 2004
Time (Months)
Dec
Nov
Oct
Sep
Aug
Jul
Jun
May
Apr
Mar
Feb
Jan
48E
55E
62E
69E
76E
83E
90E
Longitude
20
15
10
5
0
-5
-10
-15
-20
SLA

b)

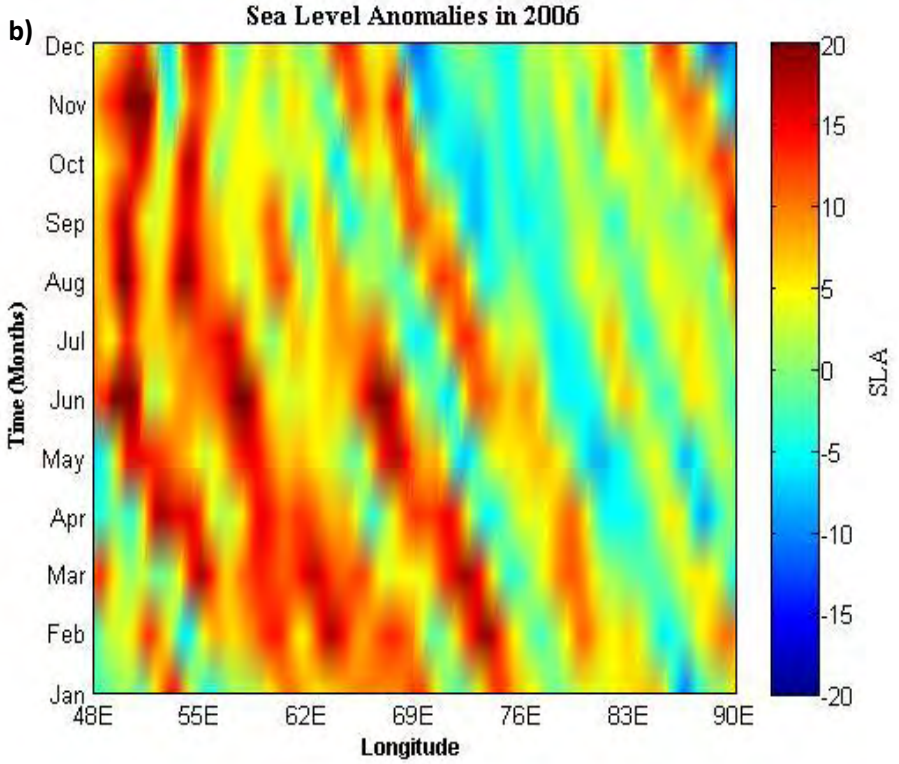
Sea Level Anomalies in 2006
Time (Months)
Dec
Nov
Oct
Sep
Aug
Jul
Jun
May
Apr
Mar
Feb
Jan
48E
55E
62E
69E
76E
83E
90E
Longitude
20
15
10
5
0
-5
-10
-15
-20
SLA

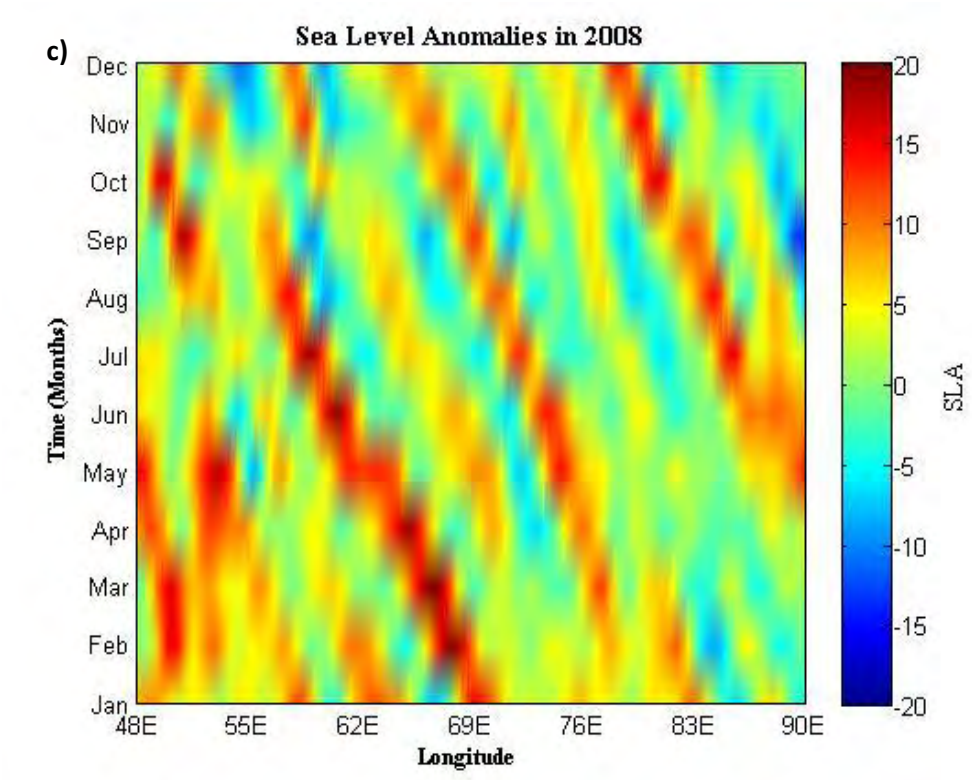


**Figure 14 Longitude time plots of SLA (cm) during a) 2004, b) 2006 and c) 2008, averaged between latitudes 24°S and 28°S.**

The spectral analysis (wavelet analysis) of Chl-a was performed in a time window of 18 months. It revealed a semi-annual signal in the southeast box and a strong annual signal in the East box. The 6-month signal was prominent during 2006 and 2008 (Figure 15). Even though there was an austral summer bloom in 2004, the wavelet analysis showed significance for a 12-month signal. This could be due to the gradual decrease of Chl-a concentration instead of a sharp decline as in 2006 and 2008. The 12-month periodicity was dominant throughout the time series, peaking in 2003-2005, 2009/2010 and 2012 onwards. The wavelet power spectrum also shows that in 2012 there was a significant semi-annual signal. In the East box, there was a persistent annual signal throughout the time period (Figure 16) with a semi-annual signal apparent (although not significant) in 2007-2009.

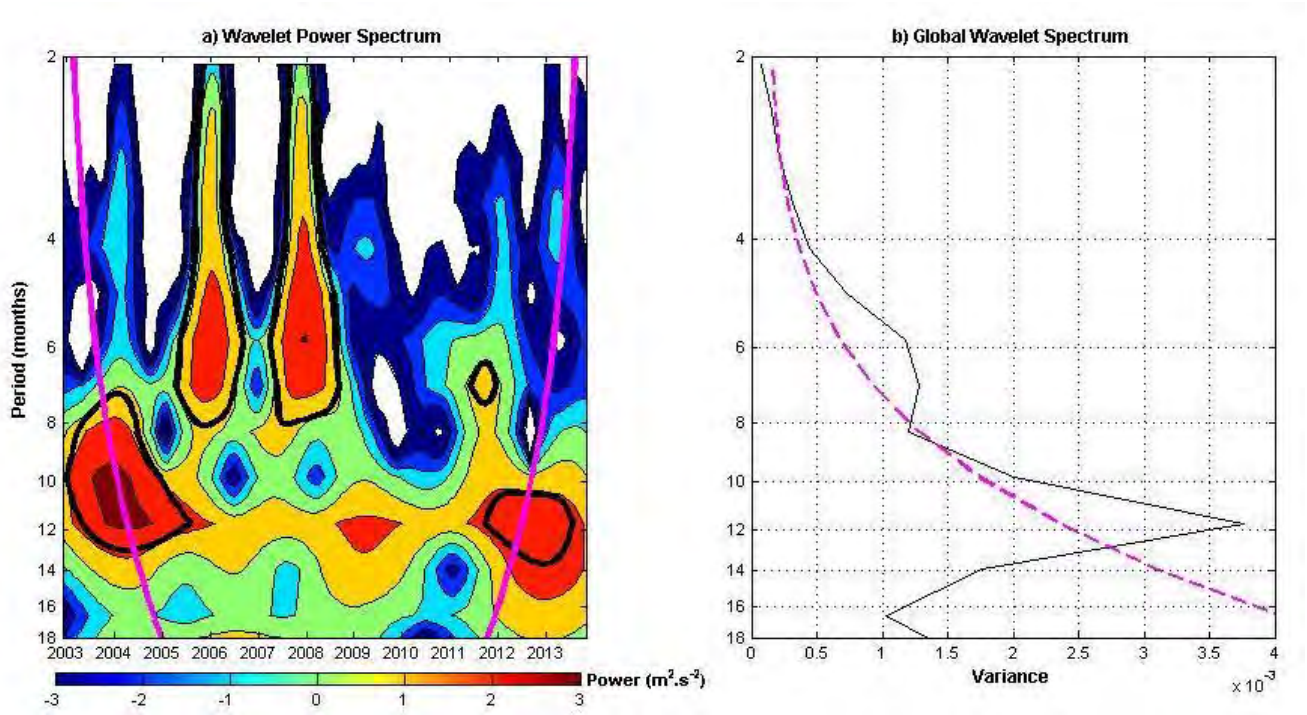


**Figure 15 Wavelet power spectrum (left) and power (right) of the wavelet analysis of Chl-a concentration over the Southeast box (48-66°E, 24-30°S). The cone of influence (COI) is indicated by the thick pink line and the black contours indicate the 95% significance levels. The thick pink dashed line in the Global wavelet spectrum represents the significance level.**

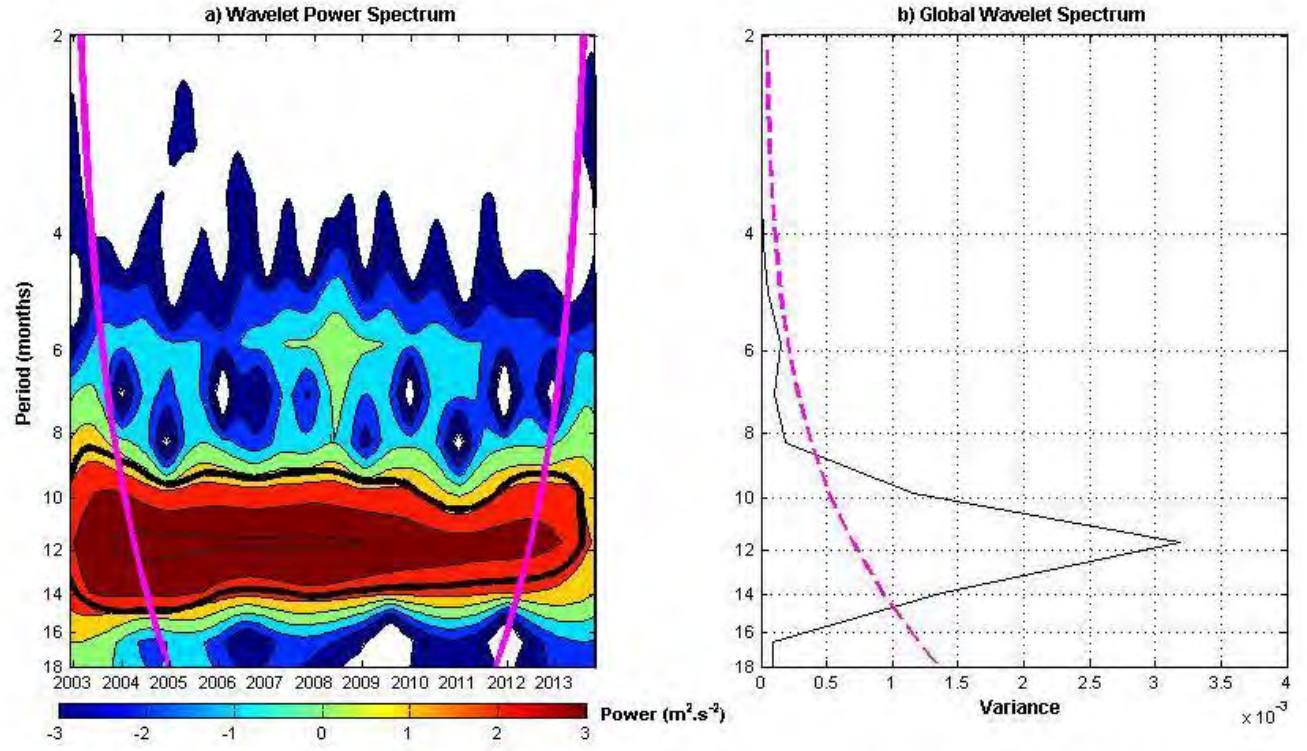


**Figure 16 Same as Figure 16 but for the East box (70-88°E, 24-30°S).**

## 5. Discussion

Along the south coast of Madagascar, an inshore upwelling cell is formed, providing the necessary conditions for the development of a bloom. The EMC prevents the bloom from propagating eastward and southward (Ho et al., 2004). Instead, the current spreads southwestward or directly westward, into the Mozambique Basin. De Ruijter et al. (2004) found a pattern that suggests a strengthening (weakening) of the EMC during La Niña (El Niño) which in turn stimulates (reduces) the vortex formation. The Chl-a is transported offshore by these mesocale eddies formed due to the EMC. The bloom which occurs east of Madagascar travels against the mean westward flow and covers a large area (~2500km) before terminating at ~70°E. The SICC acts as a meridional barrier and prevents the bloom from propagating further north and south (Huhn et al., 2012).

The seasonal cycle of the SICC is stronger in summer and weaker in winter (Palastanga et al., 2007). Around 26°S, the stronger southern part of the SICC is associated with a permanent sub-surface thermal front at 100 to 200 m depth which is present year-round, being slightly stronger during austral summer (Menezes et al., 2014). However, the jet alone cannot explain the occurrence/absence of the plankton bloom. Even though the SICC persists throughout the years, the seasonality and the inter-annual variability of the bloom do not coincide and the plankton front propagates with a higher velocity than the pure transport velocity of the jet (Huhn et al., 2012). However, the resulting persistent eastward transport caused by the jet yields support for the hypothesis of a nutrient source at the southern tip of Madagascar as the origin of the plankton bloom (Uz, 2007; Lévy et al., 2007; Raj et al., 2010; Huhn et al., 2012).

There are various hypotheses that were suggested for the possible mechanism that causes the bloom in the literature. Longhurst (2001) classified it as an ‘entrainment bloom’ caused by

mesoscale eddies whereas Srokosz et al. (2004) described it as a plankton wave originating near Madagascar which travels from west to east. Uz (2007) proposed that the bloom occurred within a shallow MLD and was caused by diazotrophic nitrogen. However, all these suggestions still remain hypotheses.

In this study, an annual cycle of Chl-a concentration was shown in Figure 6, with a maximum peak in austral winter and a minimum peak in austral summer. However, inter-annual variability exists throughout the years as seen in the time series of Chl-a. During the bloom years (2004, 2006 and 2008), the Chl-a concentration reached its maxima in summer. The bloom years identified in this study were analogous to those identified in the literature. The wavelet analysis revealed a semi-annual signal during the bloom years which coincides with the austral summer bloom in the Southeast sub-region in 2006 and 2008. In 2004, the wavelet power spectrum showed an annual signal instead of a semi-annual one. The Chl-a concentration in 2004 persisted for longer and thus did not have two distinct peaks for austral summer and winter as compared to 2006 and 2008. An annual signal was persistent throughout the dataset which coincides with the winter bloom in the East sub-region.

In the western tropical IO, the deep chlorophyll maximum (DCM) has been reported to occur at a depth between 50 and 75 m (Conkright et al., 1998; Owens et al., 1993; Wiggert et al., 2006), where it was determined by the thermocline depth, nitracline and PAR values (George et al., 2013). The Chl-a was mainly dependent on the MLD and the presence of eddies, where anti-cyclonic eddies play a major role in deepening the thermocline thus amplifying the low productivity (George et al., 2013).

Emphasis was laid on the physical conditions (SST, wind speed, geostrophic currents and SLA) at the onset of the bloom. There are slight variations in the wind speed between the two sub-regions, with the highest maxima and minima reached in the East box. However, the

variability in the wind speed does not indicate why the bloom occurred during these 3 specific years and not in others. The region at the latitude 25°S is one of enhanced sea surface height variability, with eddy and/or Rossby wave propagation westward (Quartly et al., 2006). The Hovmöller plots (Figures 14 and 17 in Appendix) reveal the mesoscale activity of the region. The study area is characterized by westward propagating anti-cyclonic and cyclonic eddies throughout the years as they are ubiquitous features of the ocean. These eddies influence the Chl-a by three different processes, namely advection of nutrients and phytoplankton either horizontally or vertically and modulation of the stratification (Gaube et al., 2014). The cyclonic and anticyclonic patterns of the mesoscale eddies can be seen in the monthly Chl-a Figures 9, 10 and 11. The Chl-a concentration is higher in the core and peripherally in cyclonic and anticyclonic eddies respectively. At the onset of the bloom, there were negative SST anomalies which could suggest that the nutrients input could be due to entrainment from below the MLD. However, they were relatively small anomalies and as the atmosphere-ocean heat fluxes in the tropical region are high (Hasternrath and Lamb, 1979) for surface water masses with lower SST anomalies (Lutjeharms and Machu, 2000) this could dissipate the SST anomaly signals. The South East sub-region is also characterized by higher EKE (Figure 19 in Appendix) which could dissipate the SST signal even more by the mixing of the surface layers. Ridderinkorf et al. (2013) found significant positive correlation between the strengths of the EMC and the EKE with the NIÑO3.4 index. After a La Niña (El Niño) event, the EMC is stronger (weaker) and there is more (less) EKE observed.

During the months of January (2005, 2011 and 2012), February (2005, 2007, 2009, 2011 and 2012), March (2007, 2009, 2010, 2012 and 2013) and April (2009, 2010, 2011 and 2013) and December (2010), the Chl-a concentration was above 0.16mg/$m^3$ even though these years were not considered as bloom years. These monthly averages are not seen in Figure 6 as there were more regions of low Chl-a in the Southeast box and thus the overall mean for these

particular months were below the threshold. A possible explanation for the high level of Chl-a could be that the Chl-a is carried away from the eastern coast, a region of higher Chl-a concentration, by the swirling motions of the eddies hitting the coast.

There are slight variations in the physical parameters in the two sub-regions, but this does not seem to explain why the bloom does not propagate further east. One possible explanation could be that by the time it takes the bloom to travel eastward, the MLD deepens with the onset of austral winter (Kara et al., 2003). Another cause could be the presence of the junction of the IO ridge systems at 25°S and ~70°E which could affect the physical processes that contribute to the eddy and MLD dynamics (Srokosz et al., 2004). Srokosz and Quartly (2013) suggested another possibility whereby the iron needed for nitrogen fixation by diazotrophs could be upwelled from the sediment near Madagascar. It is then transported eastward until the iron is exhausted, thus terminating the bloom. Since the bloom is intermittent inter-annually, its release should also vary inter-annually but no data is available till date to confirm this hypothesis (Srokosz and Quartly, 2013).

# 6. Conclusion

The SEC forms the northern boundary of the SIO subtropical gyre south of 12°S, and splits at the coast of Madagascar into NMC and EMC. The SIO is also characterized by the presence of the SICC, between 22°S and 30°S. The southward flowing EMC is a western boundary current of the South Indian subtropical gyre (Duncan, 1970; Lutjeharms, 1988b; Nauw et al., 2008) and this study focused on the inter-annual variability of the enhanced Chl-a concentration occurring east of Madagascar for a period of 11 years (2003-2013) and the physical mechanisms that control its onset, propagation and termination from satellite datasets.

The ocean colour data were used to identify the bloom as its features are more conservative than sea surface temperatures. The seasonality of Chl-a concentration generally reaches a maxima and minima in austral winter and summer respectively. However, during some years, the opposite was seen and the Chl-a concentration peaked higher than the mean level (~0.08mg/$m^3$) during the austral summers of 2004, 2006 and 2008. The timing of the onset of the austral summer bloom showed temporal and spatial variation. An active eddy field is required to develop and propagate the bloom (Longhurst, 2001; Srokosz et al., 2004). Even though the eddies are present year round, there are other factors that may affect the initiation of the bloom as it does not occur every year. The physical conditions also do not provide a clear explanation as to why the bloom occurred only during these three specific years and why it does not propagate further east, or the bloom could be present every year at the sub-surface level but is not apparent at the surface level.

## 6.1 Recommendation and future works

A more detailed analysis can be performed using the daily satellite datasets instead of the monthly datasets. However, satellite datasets for Chl-a are limited in terms of coverage due to cloud cover and thus results in large data gaps. Interpolation should be applied in time and space over the missing data. The satellite datasets only provide information on the surface of the ocean and miss a proportion of the depth-integrated Chl-a when the deep chlorophyll maximum is deeper than the first optical depth (~20m; Gordon and Mc-Cluney, 1975; Currie et al., 2013). To have a better understanding of the dynamics and the biological processes, high resolution coupled physical-biogeochemical models with higher accuracy can be used. Satellites cannot resolve eddies at the sub-mesoscale level which can have an impact on the physical and biological aspects of the upper ocean (Lévy et al., 2012).

Integrated Chl-a concentration changes are strongly related to anomalies of the depth of 20°C isotherm (Currie et al., 2013). Nutricline depths also control the changes in Chl-a and productivity on a global scale (Messié and Chavez, 2012). These can be investigated in the region of this study and they should be related to large climate modes (ENSO/IOD) as they affect the physical processes of the ocean.

# 7. Appendix

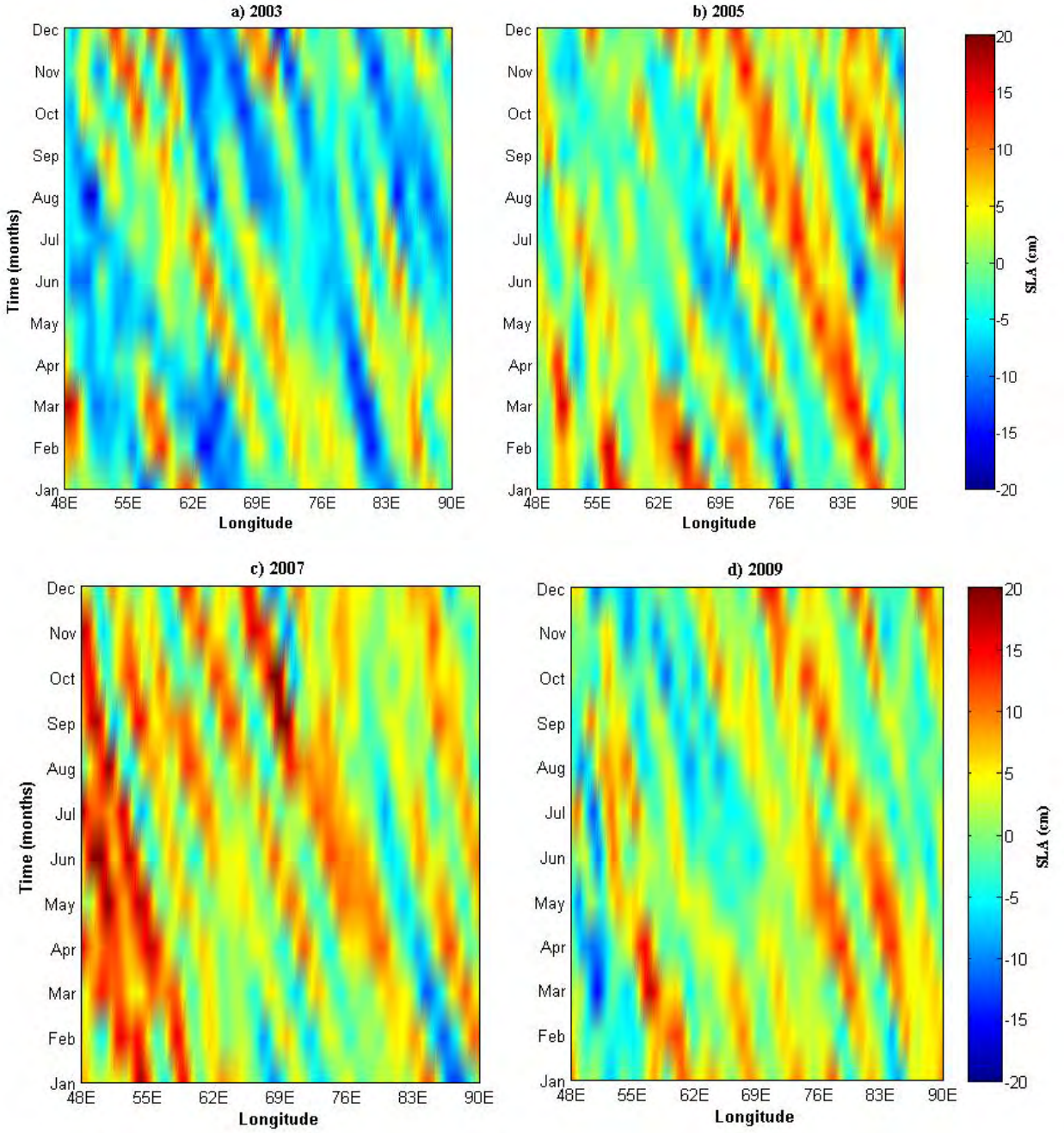
a) 2003
b) 2005
c) 2007
d) 2009
Time (months)
Longitude
SLA (cm)
Dec
Nov
Oct
Sep
Aug
Jul
Jun
May
Apr
Mar
Feb
Jan
48E
55E
62E
69E
76E
83E
90E
20
15
10
5
0
-5
-10
-15
-20

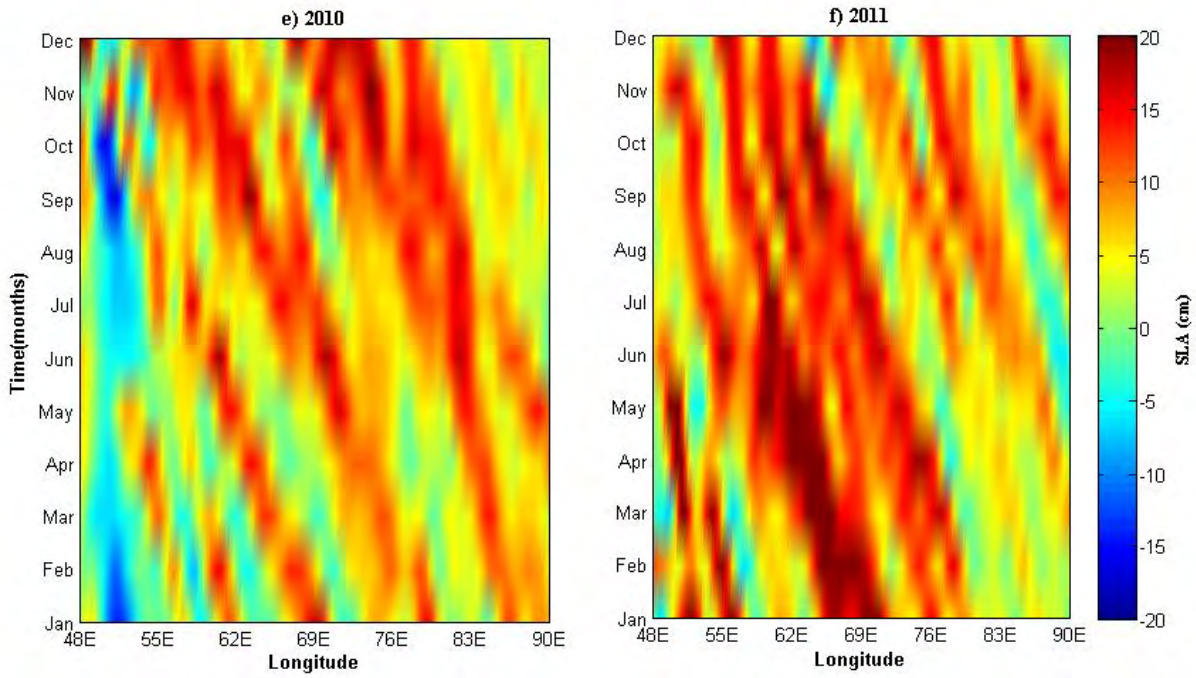


**Figure 17 Longitude time plots of SLA (cm) during the non-bloom years (a) 2003, b) 2005, c) 2007, d) 2009, e) 2010 and f) 2011) averaged between latitudes 24°S and 28°S.**

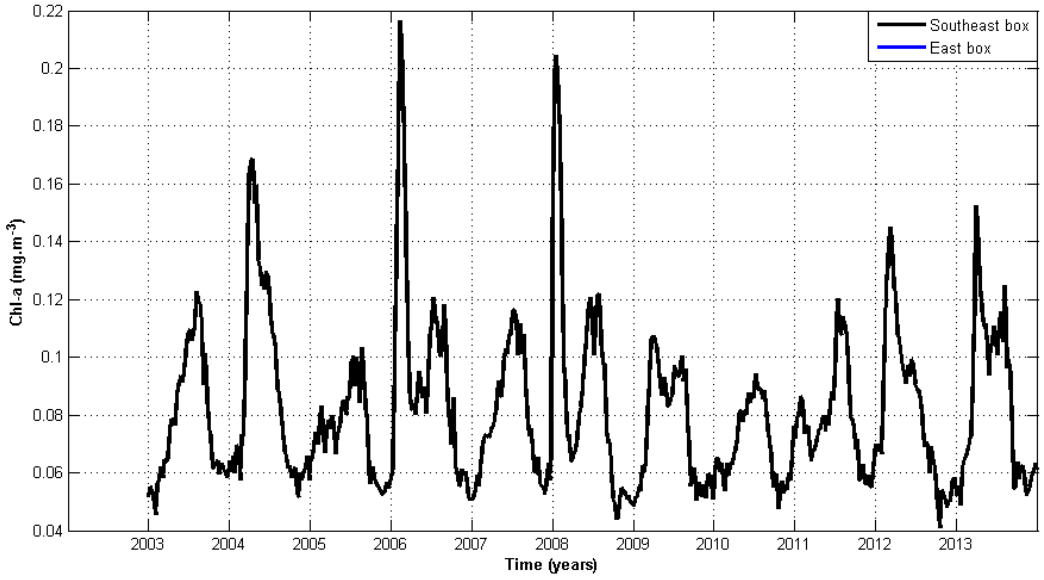


**Figure 18 Weekly time series of Chl-a concentration (mg/m$^3$) for the selected regions for the time period of 2003 to 2013.**

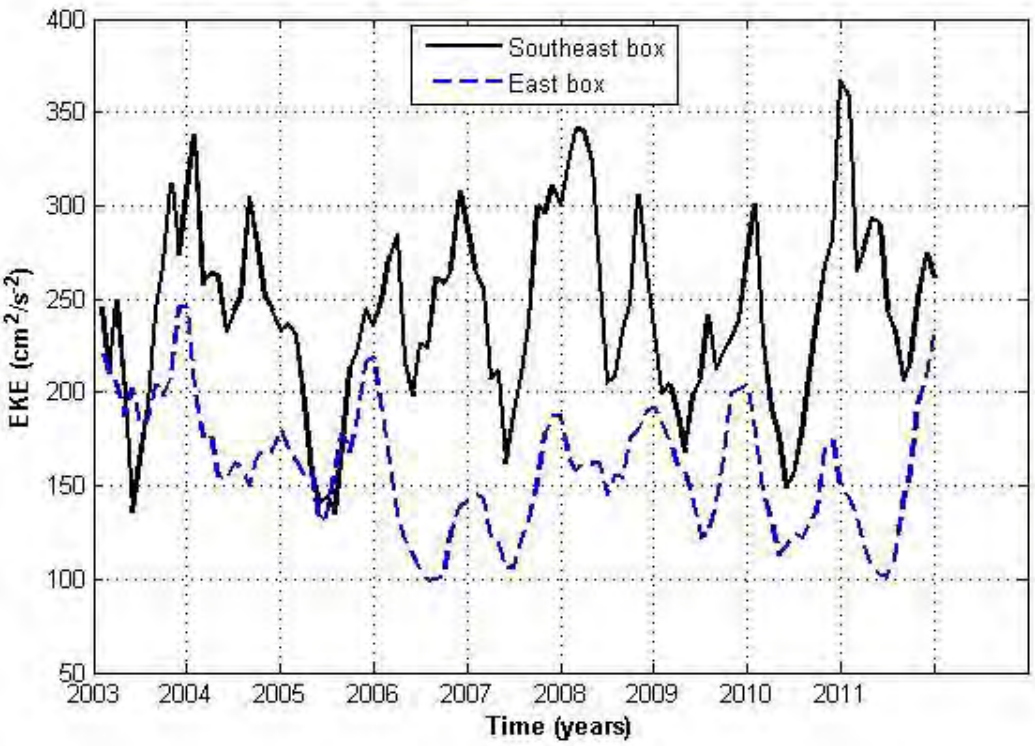


**Figure 19 Monthly time series of Eddy Kinetic Energy (EKE) (cm$^2$/s$^{-2}$) for the two sub-regions for the time period of 2003 to 2011.**

# 8. References


Battisti, D.S., and Hirst, A. C.: Interannual variability in a tropical atmosphere–ocean model: influence of the basic state, ocean geometry, and nonlinearity, Journal of Atmospheric Sciences, 46, 1687–1712, 1989.

Beal, L., de Ruijter, W., Biastoch, A., and Zahn, R.: On the role of the Agulhas system in ocean circulation and climate, Nature, 472(7344):429–436, 2011.

Beron-Vera, F. J., Olascoaga, M. J., and Goni, G. J.: Surface ocean mixing inferred from different multisatellite altimetry measurements, Journal of Physical Oceanography, 40, 2466–2480, 2010.

Beron-Vera, F. J., Brown, M. G., Olascoaga, M. J., Rypina, I. I., Koçak, H., and Udovydchenkoy, I. A.: Zonal jets as transport barriers in planetary atmospheres, Journal of Atmospheric Sciences, 65, 3316–3326, 2008.

Cai, W., Pan, A.,Roemmich, D., Cowan, T., and Guo, X.: Argo profiles a rare occurrence ofthree consecutive positive Indian Ocean Dipole events, 2006–2008, Geophysical Research Letters,36, L08701, doi: 10.1029/2008GL037038, 2009.

Cane, M. A.: The evolution of El Niño, past and future, Earth and Planetary Science Letters, 230, 227–240,2005.

Cane, M. A., Munnich, M., and Zebiak, S.E.: A study of self-excited oscillations of the tropical ocean–atmosphere system. Part 1: linear analysis, Journal of Atmospheric Sciences, 47, 1562–1577, 1990.

Chen, D., and Cane, M.A.: El Niño prediction and predictability, Journal of Computational Physics, 227, 3625-3640, doi: 10.1016/j.jcp.2007.05.014, 2008.

Chen, Z., Wu, L., Qiu, B., Sun, S., and Jia, F.: Seasonal variation of the South Equatorial Current bifurcation off Madagascar, Journal of Physical Oceanography, 44, doi: 10.1175/JPO-D-13-0147.1, 2014.

Conkright, M.E., O'Brien, T.D., Levitus, S., Boyer, T.P., Stephens, C., and Antonov, J.I.: World Ocean Atlas 1998, Nutrients and Chlorophyll of the Indian Ocean, vol. 12 of NOAA Atlas NESDIS, NODC, 1998.

Chapman, P., Di Marco, S. F., Davis, R. E., and Coward, A. C.: Flow at intermediate depths around Madagascar based on ALACE float trajectories, Deep Sea Research, Part II, 1957–1986, 2003.

Currie, J. C., Lengaigne, M., Vialard, J., Kaplan, D. M., Aumont, O., Naqvi, S. W. A., and Maury, O.: Indian ocean Dipole and El Niño/Southern Oscillation impacts on regional chlorophyll anomalies in the Indian Ocean, Biogeosciences, 10, 1-22, doi: 10.5194/bg-10-1-2013, 2013.

Daubechies, I.: Ten lectures on wavelets, CBMS-NSF, Regional Conference Series in Applied Mathematics 61, Society for Industrial and Applied Mathematics (SIAM), Philadelphia, PA, 1992.

de Ruijter, W. P.M., Brummer, G.,Drijfhout, S. S., Lutjeharms,J. R. E., Peters,F., Ridderinkhof, H., van Aken, H., and van Leeuwen, P.: Observations of the inter-ocean exchange around South Africa, Eos Transactions, American Geophysical Union, 87(9), 97–101, doi:10.1029/2006EO090002,2006.

de Ruijter, W. P. M., Ridderinkhof, H., and Schouten, M.: Variability of the southwest Indian Ocean, Philosophical Transactions of the Royal Society A, 363, 63– 76, 2005.

de Ruijter, W. P. M., van Aken, H. M., Beier, E. J., Lutjeharms, J. R. E., Matano, P. M., and Schouten, M..: Eddies and dipoles around South Madagascar: Formation, pathways and large-scale impact, Deep Sea Research, Part I, 51, 383– 400, 2004.

DiMarco, S. F., Chapman, P., Nowlin Jr., W. D., Hacker, P., Donohue, K., Luther, M., Johnson, G. C., and Toole, J.: Volume transport and property distributions of the Mozambique Channel, Deep Sea Research, Part II, 49, 1481–1511, 2002.

Duncan, C. P.: The Agulhas Current, Ph.D. thesis, 76 pp., University of Hawaii, Manoa, 1970.

Feng, M. and Meyers, G.: Interannual variability in the tropical Indian Ocean: a two-year time-scale of Indian Ocean Dipole. Deep-Sea Research Part II, Topical Studies in Oceanography, 50(12-13):2263–2284, 2003.

Flierl, G., Stern, M., and Whitehead Jr., J.: The physical significance of modons: Laboratory experiments and general integral constraints, Dynamics of Atmospheres and Oceans, 7(4), 233–263, doi: 10.1016/j.bbr.2011.03.031, 1983.

Gaube, P., McGillicuddy Jr., D. J., Chelton, D. B., Behrenfeld, M. J. and Strutton, P. G.: Regional variations in the influence of mesoscale eddies on near-surface chlorophyll, Journal of Geophysical Research: Oceans, 119, doi: 10.1002/2014JC010111, 2014.

George, J. V., Nuncio, M., Chacko, R., Anilkumar, N., Noronha, S. B., Patil, S. M., Pavithran, S., Alappattu, D. P., Krishnan, K. P., and Achuthankutty, C. T.: Role of physical processes in chlorophyll distribution in the western tropical Indian Ocean, Journal of Marine Systems, 113–114, 1–12, 2013.

Gordon, H. R., and McCluney, W. R.: Estimation of the depth of sunlight penetration in the sea for remote sensing, Applied Optics, 14, 413–416, 1975.

Gründlingh, M. L.: Tracking eddies in the southeast Atlantic and southwest Indian oceans with TOPEX/Poseidon, Journal of Geophysical Research, 100, 24977–24986, 1995.

Gründlingh, M. L.: On the winter flow in the southern Mozambique Channel, Deep Sea Research, Part I, 40, 409– 418, 1993.

Halo, I., Penven, P., Backeberg, B., Ansorge, I., Shillington, F., and Roman, R.: Mesoscale eddy variability in the southern extension of the East Madagascar Current: Seasonal cycle, energy conversion terms, and eddy mean properties, Journal of Geophysical Research: Oceans, 119, 7324–7356, doi: 10.1002/ 2014JC009820, 2014.

Hastenrath, S., and Lamb, P. J.: Climatic Atlas of the Indian Ocean. Part II: The Ocean Heat Budget, University of Wisconsin Press, Madison, xv pp., 1979.

Henson, S.A., Thomas, A. C.: Interannual variability in timing of bloom initiation in the California current system, Journal of Geophysical Research: Oceans, 112, 2007.

Hermes, J. C., Reason, C. J. C., and Lutjeharms, J. R. E.: Modeling the variability of the greater Agulhas Current system, Journal of Climate, 20, 3131–3146, doi: 10.1175/JCLI4154.1, 2007

Ho, C.-R., Zheng, Q., and Kuo, N-J.: SeaWiFs observations of upwelling south of Madagascar: long-term variability and interaction with East Madagascar Current, Deep Sea Research, Part II, 51, 59-67, doi:10.1016/j.dsr2.2003.05.001, 2004.

Huhn, F., von Kameke, A., Pérez-Muñuzuri, V., Olascoaga, M. J., and Beron-Vera, F. J.: The impact of advective transport by the South Indian Ocean countercurrent on the Madagascar bloom, Geophysical Research Letters, 39, doi:10.1029/2012GL051246, 2012.

Jin, F. F.: An equatorial ocean recharge paradigm for ENSO. Part I: conceptual model, Journal of Atmospheric Sciences, 54, 811–829, 1997.

Kantha, L. H., and Clayson, C. A.: Numerical Models of Oceans and Oceanic Processes, 940 pp., Academic Press, New York, 2000.

Kara, A. B., Rochford, P. A., and Hurlburt, H. E.: Mixed layer depth variability over the global ocean, Journal of Geophysical Research, 108(C3), 3079, doi: 10.1029/2000JC000736, 2003.

Kim, H. J., Yoo, S. J., Oh, I. S.: Relationship between phytoplankton bloom and wind stress in the sub-polar frontal area of the Japan/East Sea, Journal of Marine Systems, 67, 205–216, 2007.

Latha, T.P., Rao, K. H., Amminedu, E., Nagamani, P. V., Choudhury, S.B., Lakshmi, E., Sridhar, P.N., Dutt, C. B. S., and Dhadwal, V. K.: Seasonal variability of phytoplankton blooms in the coastal waters along the east coast of India, International Archives of the Photogrammetry, Remote Sensing and Spatial Information Sciences, XL-8, 1065-1071, doi: 10.5194/isprsarchives-XL-8-1065-2014, 2014.

Lévy, M., Ferrari, R., Franks, P., Martin, A., and Rivière, P.: Bringing physics to life at the submesoscale, Geophysical Research Letters, 39, L14602, doi: 10.1029/2012GL052756, 2012.

Lévy, M., Shankar, D., André, J.-M., Shenoi, S. S. C., Durand, F., and de Boyer Montégut, C.: Basin-wide seasonal evolution of the Indian Ocean's phytoplankton blooms, Journal of Geophysical Research, 112, C12014, doi:10.1029/2007JC004090, 2007.

Longhurst, A.: A major seasonal phytoplankton bloom in the Madagascar Basin, Deep Sea Research, Part I, 48, 2413–2422, 2001.

Lutjeharms, J. R. E., and Machu, E.: An upwelling cell inshore of the East Madagascar Current, Deep Sea Research, I, 47, 2405–2411, 2000.

Lutjeharms, J. R. E.: On the role of the East Madagascar Current as a source of the Agulhas Current, South African Journal of Science, South 84, 236-238,1988b.

Lutjeharms, J. R. E., Bang, N. D., and Duncan, C. P.: Characteristics of the currents east and south of Madagascar, Deep Sea Research, Part I, 28A, 879– 899, 1981.

Machu, E., J. R. E. Lutjeharms, A. M. Webb, and van Aken., H. M.: First hydrographic evidence of the southeast Madagascar upwelling cell, Geophysical Research Letters, 29(21), 2009, doi: 10.1029/2002GL015381, 2002.

Mahowald, N. M., Engelstaedter, S., Luo, C., Sealy, A., Artaxo P., Benitez-Nelson, C., Bonnet, S., Chen, Y., Chuang, P. Y., Cohen, D. D., Dulac, F., Herut, B., Johansen, A. M., Kubilay, N., Losno, R., Maenhaut, W., Paytan, A., Prospero, J. M., Shank, L. M., and Siefert, R. L.: Atmospheric dust deposition: Global distribution, variability and human perturbations, Annual Review of Marine Science, 1, 245–278, doi: 10.1146/annurev.marine.010908.163727, 2009.

Martin, M. V., and Shaji, C.: On the variability of thermocline depth in the Southwestern Bay of Bengal during Indian Ocean Dipole, The Climate Symposium, Darmstadt, Germany, 13-17 October, 2014.

McCarthy, M. C., and Talley, L. D.: Three-dimensional isoneutral potential vorticity structure in the Indian Ocean, Journal of Geophysical Research, 104(C6), 13,251– 13,267, 1999.

McCreary, J. P., and Anderson,D. L. T.: A simple model of El Niño and the Southern Oscillation, Monthly Weather Review, 112(5):934–946,1984.

McPhaden, M. J., Zebiak, S. E., and Glantz, M. H.: ENSO as an Integrating Concept in Earth Science, Science, 314, 1740–1745, doi:10.1126/science.1132588, 2006.

Menezes, V. V., Phillips, H. E., Schiller, A., Bindoff, N. L., Domingues, C. M., and Vianna, M. L.: South Indian Countercurrent and associated fronts, Journal of Geophysical Research: Oceans, 119, 6763– 6791, doi: 10.1002/2014JC010076, 2014

Messié, M. and Chavez, F. P.: A global analysis of ENSO synchrony: The oceans' biological response to physical forcing, Journal of Geophysical Research-Oceans, 117, C09001, doi: 10.1029/2012JC007938, 2012.

Murtugudde, R., McCreary, Jr., J. P., and Busalacchi, A. J.: Oceanic processes associated with anomalous events in the Indian Ocean with relevance to 1997–1998, Journal of Geophysical Research 105, 3295–3306, doi: 10.1029/1999JC900294, 2000.

Nauw, J. J., van Aken, H. M., Lutjeharms, J. R. E., and de Ruijter, W. P. M.: Observations of the southern East Madagascar Current and undercurrent and countercurrent system, Journal of Geophysical Research, 113, C08006, doi:10.1029/2007JC004639, 2008.

Nigam, S., and Shen, H.-S.: Structure of oceanic and atmospheric low-frequency variability over the tropical Pacific and Indian Oceans. Part I: COADS observations, Journal of Climate, 6, 657–676, 1993.

Nicholls, N.: Recent trends in the seasonal and temporal behaviour of the El Niño–Southern Oscillation, Geophysical Research Letters, 35, L19703, doi:10.1029/2008GL034499,2008.

Nicholson, S. E.: An analysis of the ENSO signal in the tropical Atlantic and western Indian Oceans, International Journal of Climatology, 17, 345–375, 1997.

Owens, N.J.P., Burkill, P.H., Mantoura, R.F.C., Woodward, E.M.S., Bellan, I.E., Aiken, J., Howland, R.J.M., and Llewellyn, C.A.: Size-fractionated primary production and nitrogen assimilation in the north western Indian Ocean, Deep Sea Research, II 40, 697–709, 1993.

Palastanga, V., Dijkstra, H. A., and de Ruijter, W. P. M.: Inertially induced connections between subgyres in the South Indian Ocean, American Meteorological Society, doi: 10.1175/2008JPO3872.1, 2009.

Palastanga, V., van Leeuwen, P. J., Schouten, M. W., and de Ruijter, W. P. M.: Flow structure and variability in the subtropical Indian Ocean: Instability of the South Indian Ocean Countercurrent, Journal of Geophysical Research, 112, C01001,doi:10.1029/2005JC003395, 2007.

Palastanga, V., van Leeuwen, P. J., and de Ruijter,W. P. M.: A link between low-frequency mesoscale eddy variability around Madagascar and the large-scale Indian Ocean variability, Journal of Geophysical Research, 111, C09029, doi:10.1029/2005JC003081, 2006.

Poulton, A. J., Stinchcombe, M. C., and Quartly,G. D.: High numbers of Trichodesmium and diazotrophic diatoms in the southwest Indian Ocean, Geophysical Research Letters, 36, L15610, doi: 10.1029/2009GL039719,2009.

Quartly, G. D., Buck, J. J. H., Srokosz, M. A., and Coward, A. C.: Eddies around Madagascar - The retroflection re-considered, Journal of Marine Systems, 63, 115– 129, 2006.

Quartly, G. D., Buck, J. J. H., and Srokosz, M. A.: Eddy variability east of Madagascar, Philosophical Transactions of the Royal Society A, 363, 77–79, 2005.

Quartly, G. D., and Srokosz, M. A.: Eddies in the southern Mozambique Channel, Deep Sea Research, Part II, 51, 69– 83, 2004.

Qiu, B., and Chen, S.: Seasonal modulations in the eddy field of the South Pacific Ocean, Journal of Physical Oceanography., 34, 1515– 1527, 2004.

Qiu, B.: Seasonal eddy field modulation of the North Pacific Subtropical Countercurrent: TOPEX/Poseidon observations and theory, Journal of Physical Oceanography., 29, 2471–2486, 1999.

Raj, R. P., Peter, B. N., and Pushadas, D.: Oceanic and atmospheric influences on the variability of phytoplankton bloom in the South western Indian Ocean, Journal of Marine Systems, 82, 217–229, 2010.

Reason, C. J. C., Allan, R. J., Lindesay, J. A., and Ansell, T. J.: ENSO and climatic signals across the Indian Ocean Basin in the global context: Part 1, Interannual composite patterns, International Journal of Climatology, 20, 1285–1327, 2000.

Rao, S. A., Behara, S. K., Masumoto, Y., and Yamagata, T.: Interannualsubsurface variability in the tropical Indian Ocean with a special emphasis on the Indian Ocean Dipole, Deep Sea Research, Part II, 49, 1549–1572, 2002.

Ridderinkhof, W., Le Bars, D., von der Heydt, A. S., and de Ruijter, W. P. M.: Dipoles of the South East Madagascar Current, Geophysical Research Letters, 40, 558–562, doi: 10.1002/grl.50157, 2013.

Rossby, H. T., Riser, S. C., and Mariano, A. J.: The western North Atlantic - A Lagrangian viewpoint, in Eddies in Marine Science, edited by A. R. Robinson, pp. 66– 91, Springer, New York, 1983.

Saji, N. H., and Yamagata, T.: Possible impacts of Indian Ocean Dipole Mode events on global climate, Climate Research, 25, 151–16, 2003.

Saji, N. H., Goswami, B. N., Vinayachandran, P. N., and Yamagata, T.: A dipole mode in the tropical Indian Ocean, Nature, 401, 360– 363, 1999.

Schmitz, W. J.: On the World Ocean Circulation, vol. 1, WHOI Technical Report, WHOI-96-03, 141 pp., Woods Hole Oceanographic Institute, Woods Hole, Mass,1996.

Schouten, M. W., de Ruijter, W. P. M., and van Leeuwen, P. J.: Upstream control of Agulhas Ring shedding, Journal of Geophysical Research, 107(C8), 3109, doi: 10.1029/2001JC000804, 2002.

Shenoi, S. S. C., Saji, P. K., and Almeida, A. M.: Near-surface circulation and kinetic energy in the tropical Indian Ocean derived from Lagrangian drifters, Journal of Marine Research, 57, 885– 907,1999.

Shuckburgh, E., Jones, H., Marshall, J., and Hill, C.: Understanding the regional variability of eddy diffusivity in the Pacific sector of the Southern Ocean, Journal of Physical Oceanography, 39, 2011–2023, 2009.

Siedler, G., Rouault, M., and Lutjeharms, J. R. E.: Structure and origin of the subtropical South Indian Ocean Countercurrent, Geophysical Research Letters, 33, L24609, doi: 10.1029/2006GL027399, 2006.

Siegel, D., Doney, S., and Yoder, J.: The North Atlantic spring phytoplankton bloom and Sverdrup's Critical Depth Hypothesis, Science, 296, 730–733, 2002.

Srokosz, M. A., and Quartly, G. D.: The Madagascar Bloom: A serendipitous study, Journal of Geophysical Research-Oceans, 118, 14–25, doi: 10.1029/2012JC008339, 2013.

Srokosz, M. A., Quartly, G. D., and Buck, J. J. H.: A possible plankton wave in the Indian Ocean, Geophysical Research Letters, 31, L13301, doi: 10.1029/2004GL019738, 2004.

Swallow, J., and Pollard, R. T.: Flow of bottom water through the Madagascar Basin, Deep Sea Research, Part I, 35, 1437– 1440, 1988.

Swallow, J., Fieux, M., and Schott, F.: The boundary currents East and North of Madagascar: 1. Geostrophic currents and transports, Journal of Geophysical Research, 93, 4951–4962, 1988.

Tomczak, M., and Godfrey, J. S.: Regional Oceanography: An Introduction, 422 pp., Elsevier, New York, 1994.

Torrence, C., and Compo, G.P.: A practical guide to wavelet analysis, Bulletin of American Meteorological Society, 79(1), 61–78, 1998.

Tourre, Y.M., and White, W.B.: ENSO signals in global upper-ocean temperature, Journal of Physical Oceanography, 25, 1317–1332, 1995.

Uz, B. M.: What causes the sporadic phytoplankton bloom southeast of Madagascar?, Journal of Geophysical Research, 112, C09010, doi:10.1029/2006JC003685, 2007.

van der Werf, P. M., Schouten, M. W.,van Leeuwen, P. J.,Ridderinkhof, H., and de Ruijter, W. P. M.: Observation and origin of an interannual salinity anomaly in the Mozambique Channel, Journal of Geophysical Research, 114(C03017), 2009.

Webster, P.J., Moore, A.M., Loschnigg, J.P., Leben, R. R.: Coupled ocean-atmosphere dynamics in the Indian Ocean during 1997–1998, Nature, 401, 356–359, 1999.

Webster, P. J., Moore,A. M.,Loschnigg, J. P., and Leben, R. R.: Thegreat Indian Ocean warming of 1997– 98: Evidence of coupled oceanic-atmospheric instabilities, Nature, 401, 356–360, 1999.

Wiggert, J. D., Murtugudde, R. G., and Christian, J. R.: Annual ecosystem variability in the tropical Indian Ocean: Results of a coupled bio-physical ocean general circulation model, Deep Sea Research, Part II, 53, 644–676, doi:10.1016/j.dsr2.2006.01.027, 2006.

Wilson, C. and Qiu, X.: Global distribution of summer chlorophyll blooms in the oligotrophic gyres, Progress in Oceanography, 78(2), 107–134, doi:10.1016/j.pocean.2008.05.002, 2008.

Winder, M., and Cloern, J. E.: The annual cycles of phytoplankton biomass, Philosophical Transactions of the Royal Society B, 365, 3215–3226,2010.

Xie, S. P., Annamalai, H., Schott, F. A., and McCreary Jr., J. P.: Structure and Mechanism of South Indian Ocean Climate Variability, Journal of Climate, 15, 864-878, 2002.

Yu, L., and Rienecker, M.M.: Mechanisms for the Indian Ocean warming during 1997–98 El Niño, Geophysical Research Letters, 26, 735–738, 1999.

Zebiak, S.E., and Cane, M. A.: A model El Niño-Southern oscillation, Monthly Weather Review, 115, 2262–2278, 1987.